

ON THE COMPUTATION OF LATTICE SUMS WITHOUT TRANSLATIONAL INVARIANCE

ANDREAS A. BUCHHEIT, TORSTEN KESSLER, AND KIRILL SERKH

ABSTRACT. This work introduces a framework for the efficient computation of oscillatory multidimensional lattice sums in geometries with boundaries, a problem intersecting pure and applied mathematics with immediate applications in condensed matter physics and topological quantum physics. The challenge in evaluating the arising sums results from the combination of singular long-range interactions with the loss of translational invariance caused by the boundaries, rendering standard tools ineffective. Our work shows that these lattice sums can be generated from a generalization of the Riemann zeta function to multidimensional non-periodic lattice sums. We put forth a new representation of this zeta function together with a numerical algorithm that ensures super-exponential convergence across an extensive range of geometries. Notably, our method's runtime is influenced only by the complexity of the considered geometries and not by the sheer number of particles, providing the foundation for efficient simulations of macroscopic condensed matter systems. We showcase the practical utility of our method by computing interaction energies in a three-dimensional crystal structure with 3×10^{23} particles. Our method's accuracy is thoroughly assessed through a detailed error analysis that both uses analytical results and numerical experiments. A reference implementation is provided online along with the article.

1. INTRODUCTION

Lattice sums and their related zeta functions are of central importance in all of mathematics, with applications ranging from the study of the distribution of prime numbers to eigenvalues of pseudo-differential operators [3]. Lattice sums that involve algebraic powers of quadratic forms allow for the description of general long-range interactions in physical systems, encompassing the Coulomb interaction between charged particles, dipolar interactions in magnetic systems, and gravitation [11]. These interactions are ubiquitous in nature and give rise to numerous applications in condensed matter and quantum physics [12, 36, 22, 38].

The interplay of long-range interactions with boundaries has important implications for fundamental research and technological application. Topological defects in magnetic materials with dipolar long-range interactions are currently being explored as building blocks in novel spintronics devices [37, 41, 45], where the material boundary needs careful consideration [35]. Topological excitations at superconductor boundaries, called Majorana zero modes, have been long-sought as the main ingredient for error-resistant quantum computing [34]. Recent results by Microsoft Quantum strongly hint at their discovery [1]. Some of the authors have recently demonstrated that exotic topological phases in unconventional superconductors can arise due to long-range interactions between electrons [9].

2010 *Mathematics Subject Classification.* Primary .

The foundation for the computation of lattice sums for complete lattices $\Lambda = AZ^d$, with $A \in \mathbb{R}^{d \times d}$ regular, is given by the Epstein zeta function, the generalization of Riemann zeta to oscillatory lattice sums in higher dimensions [20, 21]. While efficiently computable representations of this function are well established by now [15], the problem of computing lattice sums with boundaries, for instance, sums over a set $L = AN_0^d$, has remained open [17]. This work solves this long-standing issue by presenting an efficiently computable framework for lattice sums and related zeta functions of the form

$$\sum_{z \in L} \frac{e^{-2\pi i \mathbf{y} \cdot \mathbf{z}}}{|\mathbf{z}|^\nu}, \quad \operatorname{Re}(\nu) > d,$$

with $\mathbf{y} \in \mathbb{R}^d$, including their meromorphic continuations to $\nu \in \mathbb{C}$ for a large set of geometries L . We focus on recombinations of the corner $L = AZ^d - \mathbf{x}$ with $\mathbf{x} \in \mathbb{R}^d$, including parallelepipeds and half-spaces, from which all relevant crystal structures can be constructed.

This work is designed for an interdisciplinary audience with diverse aims and backgrounds. Consequently, we have structured it as follows. In Section 2, we discuss the Epstein zeta function for complete lattices and present a compact reformulation of Crandall's formula that allows for its efficient evaluation. Section 3 presents the main results for general point sets L and provides all the necessary tools for applying our method. After introducing a generalized Crandall formula for zeta functions on uniformly discrete sets, we present an efficiently computable representation for prototypical lattice subsets, including corners and parallelepipeds. In Section 4, we benchmark the performance of our method and compute energies in a macroscopic 3D crystal structure of physical relevance, incorporating nontrivial boundaries. We provide the full source code alongside the article to facilitate the application of our method by readers. Our conclusions and an outlook on future applications are presented in Section 5. Section 6 details the derivation of the generalized Crandall formula. The detailed algorithm for numerically computing the zeta functions is laid out in Section 7. Finally, Section 8 benchmarks our results against analytical results and numerical experiments. Proofs of technical lemmas are provided in the appendix. A reference implementation of our algorithm together with a notebook that generates the figures of this articles is available at <https://doi.org/10.5281/zenodo.10783201>.

2. EPSTEIN ZETA AND REFORMULATION OF CRANDALL'S FORMULA

We begin by introducing the concept of lattices.

Definition 2.1 (Lattices). A lattice $\Lambda \subseteq \mathbb{R}^d$ is defined as a periodic set of points of the form $\Lambda = AZ^d$, with $A \in \mathbb{R}^{d \times d}$ regular. An important property of the lattice is its elementary lattice cell volume $V_\Lambda = |\det A|$.

The central mathematical object of study in the description of long-range lattice sums is the Epstein zeta function.

Definition 2.2 (Epstein zeta function). Let $\Lambda = AZ^d$, with $A \in \mathbb{R}^{d \times d}$ regular, $\mathbf{x}, \mathbf{y} \in \mathbb{R}^d$, and $\nu \in \mathbb{C}$. Then for $\operatorname{Re}(\nu) > d$, the Epstein zeta function is defined by the Dirichlet series

$$Z_{\Lambda, \nu} \left| \begin{array}{c} \mathbf{x} \\ \mathbf{y} \end{array} \right| = \sum_{z \in \Lambda} \frac{e^{-2\pi i \mathbf{y} \cdot \mathbf{z}}}{|\mathbf{z} - \mathbf{x}|^\nu},$$

where the primed sum excludes the case $\mathbf{x} = \mathbf{z}$. The function is meromorphically continued to $\nu \in \mathbb{C}$.

Originally introduced at the beginning of the 20th century by Paul Epstein [20, 21], it forms the natural generalization of the Riemann zeta function to oscillatory singular lattice sums in higher dimensions. Its applications span from the computation of electrostatic crystal potentials [18, 19], over analytic number theory and statistical mechanics [42], to quantum field theory [17]. Two of the authors have recently developed the Singular Euler–Maclaurin expansion (SEM), a generalization of the 300-year-old Euler–Maclaurin summation formula to singular functions in higher dimensions [7, 8] that uses the Epstein zeta function as a key element. This method has led to the prediction of two new phases in unconventional superconductors [10].

Starting with early works by Chowla and Selberg [14], Terras [43], Shanks [39], and Elizalde [16], exponentially convergent series expansion that allow for the efficient evaluation of the Epstein zeta function in any dimension have been developed. A combination of Mellin transform and Poisson summation yields Crandall’s formula [15], constituting the most modern approach. Here, we compactly reformulate it as follows.

Theorem 2.3 (Crandall’s formula). *Let $\Lambda = AZ^d$ with $A \in \mathbb{R}^{d \times d}$ regular, $\mathbf{x}, \mathbf{y} \in \mathbb{R}^d$, and $\nu \in \mathbb{C} \setminus \{d\}$. Then for any $\lambda > 0$,*

$$Z_{\Lambda, \nu} \left| \begin{array}{c} \mathbf{x} \\ \mathbf{y} \end{array} \right| = \frac{(\lambda^2/\pi)^{-\nu/2}}{\Gamma(\nu/2)} \left(\sum_{\mathbf{z} \in \Lambda} G_\nu((\mathbf{z} - \mathbf{x})/\lambda) e^{-2\pi i \mathbf{y} \cdot \mathbf{z}} + \frac{\lambda^d}{V_\Lambda} \sum_{\mathbf{k} \in \Lambda^*} G_{d-\nu}(\lambda(\mathbf{y} - \mathbf{k})) e^{-2\pi i \mathbf{x} \cdot (\mathbf{y} - \mathbf{k})} \right),$$

with the reciprocal lattice $\Lambda^* = A^{-T}Z^d$. The function G_ν is defined as

$$G_\nu(\mathbf{z}) = \frac{\Gamma(\nu/2, \pi \mathbf{z}^2)}{(\pi \mathbf{z}^2)^{\nu/2}} = \int_{-1}^1 |t|^{-\nu} e^{-\pi \mathbf{z}^2/t^2} \frac{dt}{|t|}, \quad \mathbf{z} \in \mathbb{R}^d \setminus \{\mathbf{0}\},$$

and $G_\nu(\mathbf{0}) = -2/\nu$. Here $\Gamma(\nu, z)$ denotes the upper incomplete Gamma function.

Due to the super-exponential decay of G_ν , summation both in real and in reciprocal space can be restricted to lattice elements close to $\mathbf{0}$, allowing for an efficient and precise numerical evaluation.

The effectiveness of Crandall’s formula is based on Poisson summation, which fundamentally utilizes the periodicity of the lattice, which means that if $\mathbf{z} \in \Lambda$, then $\mathbf{z} + \Lambda = \Lambda$. A significantly more challenging task arises when the summation is restricted to a non-translationally invariant subset L of a lattice, for instance $L = \mathbb{N}^d \subseteq \mathbb{Z}^d$. The resulting zeta functions are of central importance in high-energy physics and frequently appear in the zeta function regularization method for path integrals developed by Hawking [29]. Computing these lattice sums is a well-known hard problem, for which, so far, only asymptotic expansions in the specific case $L = \mathbb{N}^2$ have been developed [17]. Only few analytic results for such lattice sums have been derived to date, most notably by Glasser and Zucker [27, 46].

In this work we solve this long-standing problem by providing an exponentially convergent series representation of the arising zeta functions for a vast range of lattice subsets, including corners and parallelepipeds.

3. MAIN RESULT: COMPUTING NON-TRANSLATIONALLY INVARIANT LATTICE SUMS

The periodicity of lattices forbids the presence of boundaries. Hence, in order to describe realistic finite material structures, a more general concept is needed, namely uniformly discrete sets.

Definition 3.1 (Uniformly discrete sets). Let $L \subseteq \mathbb{R}^d$. The set L is said to be uniformly discrete if there exists $\varepsilon > 0$ such that the Euclidean distance between any two distinct points $\mathbf{x}, \mathbf{y} \in L$ satisfies $|\mathbf{x} - \mathbf{y}| > \varepsilon$.

In this section, we provide a general framework for computing oscillatory sums over uniformly discrete sets $L \subseteq \mathbb{R}^d$ as described by the following zeta function.

Definition 3.2 (Set zeta function). Let $L \subseteq \mathbb{R}^d$ be uniformly discrete, $\mathbf{y} \in \mathbb{R}^d$, and $\nu \in \mathbb{C}$ with $\operatorname{Re}(\nu) > d$. We then define the set zeta function

$$Z_{L,\nu}(\mathbf{y}) = \sum_{\mathbf{z} \in L} \frac{e^{-2\pi i \mathbf{y} \cdot \mathbf{z}}}{|\mathbf{z}|^\nu}.$$

Note that the zeta function for the set L is immediately related to the Epstein zeta function if L is a shifted lattice.

Remark 3.3. Let $L \subseteq \mathbb{R}^d$ be a lattice. Then the Epstein zeta function and the zeta function for the uniformly discrete set $L - \mathbf{x}$ with $\mathbf{x} \in \mathbb{R}^d$ are connected as follows,

$$Z_{L,\nu} \left| \begin{array}{c} \mathbf{x} \\ \mathbf{y} \end{array} \right| = e^{-2\pi i \mathbf{y} \cdot \mathbf{x}} Z_{L-\mathbf{x},\nu}(\mathbf{y}).$$

By the above equality, we extend the definition of the Epstein zeta function to arbitrary uniformly discrete sets L .

Note that the set zeta function does not require an additional parameter \mathbf{x} , compared to the Epstein zeta function, rendering the presentation more condensed. This work will put its focus on the particularly important case that L is a shifted subset of a lattice, $L + \mathbf{x} \subseteq \Lambda$, with $\mathbf{x} \in \mathbb{R}^d$. The theory that we build, however, applies to arbitrary uniformly discrete sets.

Our work is based on the theory of tempered distributions, which we review in Section 6.1. In this context, the Fourier transform is defined as follows.

Definition 3.4 (Fourier transformation). For an integrable function $f : \mathbb{R}^d \rightarrow \mathbb{C}$ the Fourier transformation $\mathcal{F}f = \hat{f}$ is given by

$$\hat{f}(\boldsymbol{\xi}) = \int_{\mathbb{R}^d} f(\mathbf{x}) e^{-2\pi i \mathbf{x} \cdot \boldsymbol{\xi}} d\mathbf{x}, \quad \boldsymbol{\xi} \in \mathbb{R}^d.$$

This definition is then extended to tempered distributions by duality. Of particular importance in our treatment are discrete measures.

Definition 3.5 (Generalized Dirac comb and form factor). Let $L \subseteq \mathbb{R}^d$ be uniformly discrete. We define the generalized Dirac comb for L as

$$\mathbf{1}_L = \sum_{\mathbf{z} \in L} \delta_{\mathbf{z}},$$

with $\delta_{\mathbf{z}}$ the Dirac delta distribution. The generalized Dirac Comb then defines a tempered distribution, whose Fourier transformation $\hat{\mathbf{1}}_L$ is called the form factor. Of particular importance is the set $L^* = \operatorname{sing\,supp} \hat{\mathbf{1}}_L$, outside of which the form factor can be identified by a smooth function.

Equipped with the form factor $\hat{\mathbf{1}}_L$, we now present the first main result of this work, the generalized Crandall formula for set zeta functions.

Theorem 3.6 (Set zeta Crandall). *Let $L \subseteq \mathbb{R}^d$ be uniformly discrete and $\mathbf{y} \in \mathbb{R}^d \setminus L^*$. Then $Z_{L,\nu}(\mathbf{y})$ can be extended to a meromorphic function in $\nu \in \mathbb{C}$ via the representation*

$$Z_{L,\nu}(\mathbf{y}) = \frac{\pi^{\nu/2}}{\lambda^\nu \Gamma(\nu/2)} \left(\sum'_{\mathbf{z} \in L} e^{-2\pi i \mathbf{y} \cdot \mathbf{z}} G_\nu(\mathbf{z}/\lambda) + \lambda^d \left(\hat{\mathbf{1}}_L * G_{d-\nu}(\lambda \cdot) \right) (\mathbf{y}) \right).$$

For fixed ν , $Z_{L,\nu}$ is smooth on $\mathbb{R}^d \setminus L^*$.

Similar to the Crandall formula in Theorem 2.3, the sum is split into a contribution in real space and a contribution in Fourier space. The computation of the real space sum is simple due to the superexponential decay of G_ν , which allows us to suitably truncate the sum. The difficulty in computing the zeta function thus lies in the computation of the convolution in Fourier space. We approach this challenge by first transforming it into a one-dimensional integral involving an ν -independent function.

Theorem 3.7 (Hadamard integral representation). *For $\mathbf{y} \in \mathbb{R}^d \setminus L^*$, the convolution in Theorem 3.6 admits the analytic representation*

$$\frac{1}{\Gamma(\nu/2)} \left(\hat{\mathbf{1}}_L * G_{d-\nu} \right) (\mathbf{y}) = \frac{2}{\Gamma(\nu/2)} \int_0^1 t^{\nu-d-1} \psi_L(t/\lambda, \mathbf{y}) dt,$$

with $\psi_L \in C^\infty([0, 1] \times (\mathbb{R}^d \setminus L^*))$,

$$\psi_L(t, \mathbf{y}) = \left(\hat{\mathbf{1}}_L * e^{-\pi \cdot^2 / t^2} \right) (\mathbf{y}), \quad t > 0,$$

and smoothly extended to $t = 0$. Furthermore, the right hand side is a smooth function outside L^* for any $\nu \in \mathbb{C}$.

Here, the dashed integral denotes the meromorphic continuation of the integral to $\nu \in \mathbb{C}$, referred to as the Hadamard integral, see [25]. The formula for ψ_L can be related to a generalization of the Faddeeva function, which is explained in more detail in Section 7.2.

Under the condition that we can efficiently compute both ψ_L and the Hadamard integral, the above formula serves as the basis for the computation of the set zeta function. Our focus now narrows to the particularly important case where L is a shifted subset of a lattice Λ with boundaries, which we refer to as lattice cuts. The prototypical geometry, from which all relevant lattice cuts can be generated, is the corner $L = A\mathbb{N}_0^d - \mathbf{x}$ with $\mathbf{x} \in \mathbb{R}^d$.

Theorem 3.8. *Let $L = A\mathbb{N}_0^d - \mathbf{x}$, with $\mathbf{x} \in \mathbb{R}^d$. Theorem 3.6 then extends to $\mathbf{y} \in L^*$, with*

$$L^* \subseteq \{ \mathbf{y} \in \mathbb{R}^d : A^T \mathbf{y} \text{ has at least one integer component} \},$$

where the corresponding zeta function is meromorphic in ν with simple poles at $\nu \in (d - \mathbb{N}_0) \setminus (-2\mathbb{N}_0)$.

Computing ψ_L and thus the zeta function for a non-translationally invariant set is a challenging task. We overcome this obstacle and demonstrate in this work that for $L = A\mathbb{N}_0^d - \mathbf{x}$, it is possible to efficiently evaluate ψ_L in any number of space dimensions and thus the related zeta function. This result immediately allows for

the computation of general lattice subsets, such as half-planes and parallelepipeds. This is achieved by means of a non-oscillatory integral representation of ψ_L .

Theorem 3.9 (Integral representation of ψ_L). *Consider $L = A\mathbb{N}_0^d - \mathbf{x}$ with $\mathbf{x} \in A^{-T}\mathbb{R}_{<0}^d$, and $\mathbf{y} \in \mathbb{R}^d$. Then ψ_L admits an efficiently computable representation, which reads for $t > 0$,*

$$\psi_L(t, \mathbf{y}) = e^{2\pi i \langle \mathbf{y}, \mathbf{x} \rangle} e^{-\pi |t\mathbf{x}|^2} \frac{t^d}{\bar{V}_\Lambda} \int_{\mathbb{R}^d} \frac{e^{-\pi(A^{-T}\boldsymbol{\xi})^2}}{\prod_{j=1}^d (1 - e^{-2\pi it(\boldsymbol{\xi} - \mathbf{Y}(t))_j})} d\boldsymbol{\xi},$$

where

$$\mathbf{Y}(t) = -A^T(\mathbf{y}/t + i\mathbf{x}).$$

For all $\mathbf{y} \in \mathbb{R}^d$ and $t > 0$, the function ψ_L can be analytically continued to $\mathbf{x} \in \mathbb{R}^d$.

A detailed description of the algorithm used to compute the zeta function for the corner is provided in Section 7. Here, we discuss how to choose the splitting parameter λ , compute the Hadamard integral efficiently, and form the analytic continuation of ψ_L .

We can construct set zeta functions for numerous geometries from the corner through suitable recombination. The most important case is the parallelepiped.

Corollary 3.10 (Parallelepiped zeta function). *The zeta function for a parallelepiped-shaped sublattice $L = A \prod_{j=1}^d \{0, 1, \dots, n_j - 1\} - \mathbf{x}$ with $\mathbf{x} \in \mathbb{R}^d$ and $\mathbf{n} \in \mathbb{N}_0^d$ can be expressed as a sum of zeta functions for corner cuts,*

$$Z_{L, \nu}(\mathbf{y}) = \sum_{\boldsymbol{\alpha} \in \{0, 1\}^d} (-1)^{\boldsymbol{\alpha}} Z_{L_0 + A\mathbf{c}_\alpha, \nu}(\mathbf{y}),$$

with $L_0 = A\mathbb{N}_0^d - \mathbf{x}$, and $(\mathbf{c}_\alpha)_j = 0$ if $\alpha_j = 0$ and $(\mathbf{c}_\alpha)_j = n_j$ if $\alpha_j = 1$.

Proof. In view of

$$L = A \prod_{j=1}^d (\mathbb{N}_0 \setminus (\mathbb{N}_0 + n_j)) - \mathbf{x},$$

the indicator function of the parallelepiped can be written as a sum of indicator functions of corners

$$\mathbb{1}_L = \sum_{\boldsymbol{\alpha} \in \{0, 1\}^d} (-1)^{\boldsymbol{\alpha}} \mathbb{1}_{L_0 + A\mathbf{c}_\alpha},$$

from which the statement readily follows due to linearity of convolution and Fourier transform. \square

Recombination of corners and parallelepipeds then yields general geometries. By introducing an integral representation of ψ_L for the corner geometry in Theorem 3.9 that is non-oscillatory and thus numerically tractable, we transform our theoretical insights into an efficient numerical framework. By constructing arbitrary geometries from simple corner units through recombination, we offer a flexible approach for treating general lattice subsets. As a result, our method is universally applicable across any interaction exponent ν , wave vector \mathbf{y} , spatial dimension d , and for an extensive range of geometries. We now benchmark the performance of our method in a physically relevant example.

4. NUMERICAL APPLICATION: BOUNDARY EFFECTS IN A MACROSCOPIC 3D SPIN STRUCTURE

Spin systems with long-range interactions hold enormous technological potential. Defects inside these materials could be used as information carriers in spintronics devices, allowing for higher storage capacities, faster computations, and lower energy consumption compared to conventional semiconductor electronics [23]. In fundamental physics, spin-ice materials have been discovered where defects behave like magnetic monopoles [12, 4]. The long-range dipolar interaction is highly important in their formation, leading to an effective Coulomb interaction between the monopoles [6]. It has recently been shown that power-law interactions between spins can be artificially created in a laboratory by placing them inside a cavity, an arrangement of highly reflective mirrors that strongly enhances laser light, where laser photons mediate an effective interaction between spins [24]. These experiments can be used to simulate exotic phases of quantum matter such as superconductors, materials that exhibit no electric resistance and can transport electric current over arbitrary distances. Some of the authors have recently shown that long-range interactions can give rise to exotic topological phases in superconductors that have non-trivial behavior at the boundary [9]. However, the computation of the long-range interactions in three dimensions with an interaction exponent ν close to the system dimension, i.e., the dipolar interaction, is well-known to be notoriously difficult [5].

We now apply our method to the computation of long-range interaction energies in a macroscopic three-dimensional crystal geometry with non-trivial boundaries. Our geometry of choice is a macroscopic spin circuit, see Fig. 1 (a), defined by the domain

$$\Omega = \{\mathbf{x} \in \mathbb{R}^3 : L/4 \leq |x_1| + |x_2| \leq L/2, |x_3| \leq L/40\},$$

with L the outer edge length. Microscopically, the crystal is composed of atoms arranged in a cubic lattice structure, $L = \Omega \cap \Lambda$, with $\Lambda = a\mathbb{Z}^3$, see Fig. 1 (b). Each atom shall carry a magnetic moment or spin $\mathbf{S}(\mathbf{x})$, described by a three-dimensional vector of unit norm (blue arrows). Choosing a lattice constant $a = 10^{-10}$ m and $L = 2 \times 10^8 a$, our geometry has a macroscopic size with an outer edge length of 2 cm, an inner edge length of 1 cm, and a height of 1 mm. In total, the structure includes more than 3×10^{23} particles.

The interaction energy of the spin at position \mathbf{x} with all surrounding spins due to an antiferromagnetic power-law long-range interaction with exponent ν is given by

$$U(\mathbf{x}) = \sum'_{\mathbf{z} \in L} \frac{\mathbf{S}(\mathbf{x}) \cdot \mathbf{S}(\mathbf{z})}{|\mathbf{x} - \mathbf{z}|^\nu},$$

with position measured in units of a and energy measured in terms of interaction energy of two neighboring spins. We now assume that all spins are aligned in the x_3 direction and subsequently introduce a prototypical defect at position $\mathbf{x} \in L$ by inverting the corresponding spin orientation $\mathbf{S}(\mathbf{x}) \rightarrow -\mathbf{e}_3$. The interaction energy due to long-range interactions of this defect as a function of position can then be computed from the generalized zeta function for the spin circuit. The energy as a function of position on the symmetry plane $x_3 = 0$ is displayed in Fig. 1 (c) for the particularly challenging case $\nu = 3$ (including a small positive offset of 10^{-3}). Interactions of this kind include the isotropic part of the dipole interaction and light-induced long-range interactions in optical cavities [24]. Additional contours close to the energy minimum are highlighted.

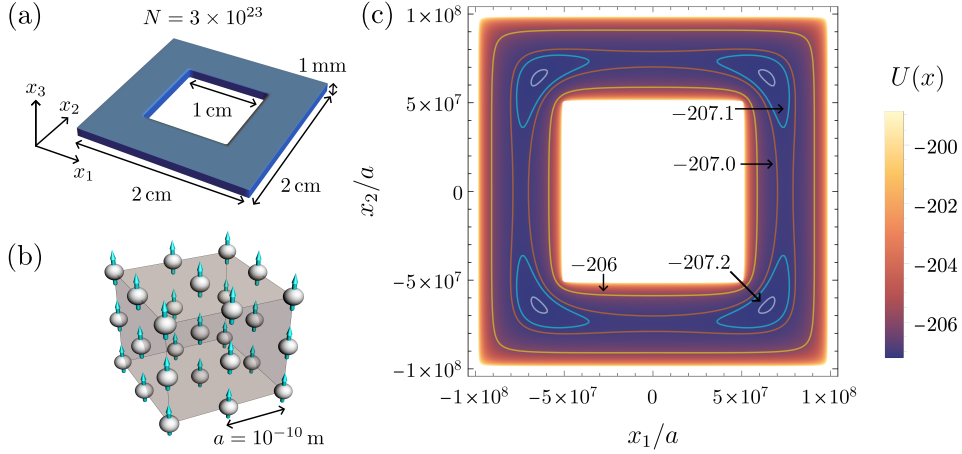


FIGURE 1. (a) Schematic depiction of a macroscopic three-dimensional spin circuit with inner edge length 1 cm, outer edge length 2 cm, and thickness 1 mm. (b) Microscopic structure with spins (blue arrows) polarized in the x_3 direction. The material exhibits a cubic lattice structure and lattice constant $a = 10^{-10}$ m, amounting to $N = 3 \times 10^{23}$ particles in total. (c) Potential energy due to long-range interactions with exponent $\nu = 3.001$ of a spin defect obtained from inverting the spin orientation as a function of position $\mathbf{x} = (x_1, x_2, 0)^T$ with $x_3 = 0$ corresponding to the symmetry plane. Position is written in units of the lattice constant and potential energy in units of the interaction energy of neighboring parallel spins. Additional contours close to the energy minimum are highlighted at values -206 (yellow), -207.0 (orange), -207.1 (blue), and -207.2 (white). The figure excludes the immediate boundary layer, where the potential energy increases sharply.

We find that the minimum energy is reached in four points in the material, inside the white contours. The energy increases when approaching the boundary, with sharp features appearing at the edges and corners. The immediate boundary layer, where the energy increases sharply, is excluded from the plot for better visualization. Surprisingly, for an exponent ν close to the system dimension, the potential is not flat inside the crystal, but the presence of the boundary has an effect even on macroscopic scales. This is visualized by the different contours at energies -206 (yellow), -207.0 (orange), -207.1 (blue), and -207.2 (white). This means that it is impossible to describe the material by its bulk properties only, and boundary effects always need to be included, not only for mesoscopic systems but also at macroscopic scales. Another important conclusion from our results is that long-range interactions tend to repel defects away from the boundary and localize them in the center of the material. This is highly relevant for magnetic defects as information carriers, as they can be destroyed at the boundary, which is a significant problem in technological applications [35]. Our numerical experiment thus shows that long-range interactions can give rise to repelling boundaries that protect defects from boundary annihilation.

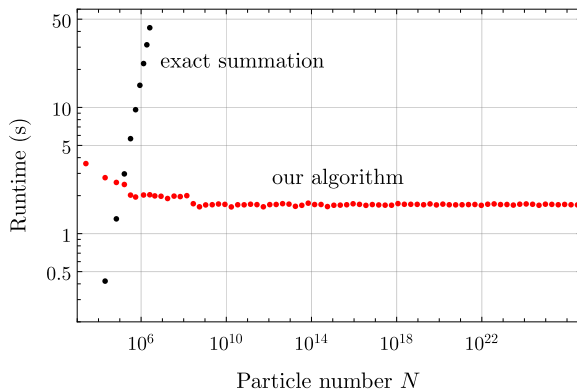


FIGURE 2. Runtime for evaluating the potential energy for introducing a defect in the spin circuit as a function of particle number N . Particle number is modified by rescaling the geometry while keeping the lattice constant fixed. While the numerical effort for exact summation increases linearly (black), our approach (red) yields an effectively constant runtime even up to macroscopic particle numbers.

They can even localize defects in certain regions of the geometry, in this case within the white contours.

For a macroscopic structure of this size, reference computations using exact summation are impossible, as the evaluation of a single energy evaluation requires to compute a sum with 3×10^{23} summands. In order to still be able to quantify the precision of our approach, we benchmark our results on a rescaled geometry with $L = 160a$, which amounts to $N \approx 1.5 \times 10^5$ particles. We compare our approach with exact summation on L using an equidistant grid with lattice constant $4a$ on the surface $x_3 = 0$. The maximum relative error of the energy then equals 1.2×10^{-12} . Our algorithm achieves full precision, up to the condition number of the problem, for the full parameter range, as verified in Section 8.

The main advantage of our method lies in a numerical effort that solely depends on the complexity of the geometry and not on the particle number. We benchmark this claim by evaluating the time required to evaluate $U(\mathbf{x})$ at the position $\mathbf{x} = (-L/4, -L/4, 0)^T$ while rescaling the geometry through rescaling the parameter L , making sure that \mathbf{x} remains a lattice point. In Fig. 2, we display the single-core runtime for evaluating the energy as a function of the rescaled particle number on an Apple M1 Max processor. We observe that while the runtime for exact summation increases linearly (black points), our algorithm (red) offers a runtime that is essentially independent of the number of particles. For macroscopic particle numbers, evaluating the lattice sum amounts to a runtime of less than 2 seconds. The runtime even decreases slightly as the particle number increases, as the crystal boundaries move away from each other, allowing for a slightly faster evaluation of the arising zeta functions.

5. OUTLOOK AND CONCLUSIONS

Algorithms for calculating zeta functions on lattices with boundaries have been highly sought after. However, until now, only asymptotic expansions for the 2D corner geometry \mathbb{N}_0^2 have been developed [17]. The present work solves this long-standing challenge. For any dimension, any interaction exponent, and any lattice, we present an efficiently computable representation of zeta functions for lattice subsets, focusing specifically on corners and parallelepipeds. We demonstrate that our approach enables the precise and rapid computation of energies in long-range interacting lattice systems with as many as 3×10^{23} particles and non-trivial boundaries, yielding results of significance for spintronics applications in less than two seconds on a standard laptop. While the computational cost of calculating the exact sum increases linearly with the number of particles, the computational effort for our method is constant. Its complexity depends only on the structures formed by the particles and not on their number, thereby facilitating precise and efficient simulations of macroscopic particle systems.

In future work, we plan to apply this method to analyze long-range interacting systems in condensed matter and quantum physics. We are particularly interested in boundary effects in superconductors, for example, topological excitations such as Majorana fermions, which are promising for use as error-resistant qubits. Further development of our method will explore generalizations of lattices where periodicity is no longer a given, with quasi-crystals as an initial focus to probe new physical effects in generalized point structures.

6. DERIVATION

In this section, we provide the proofs for the results in the main section. After providing standard results in Section 6.1, we derive the generalized Crandall formula for set zeta functions in Section 6.2. The Hadamard integral representation for the convolution part is derived in Section 6.3 and the efficiently computable integral representation for the corner geometry is discussed in Section 6.4.

6.1. Preliminaries. We first collect results from the theory of distributions that are needed for the treatment of general lattice sums. We begin with the definition of the spaces involved [31].

Definition 6.1 (Test functions and distributions). For an open set $\Omega \subseteq \mathbb{R}^d$, we denote the space of smooth test function with compact support on Ω by $\mathcal{D}(\Omega)$. Its dual space, called the space of distributions, is written as $\mathcal{D}'(\Omega)$.

Definition 6.2 (Functions of superalgebraic decay). For $k \in \mathbb{N} \cup \{\infty\}$, $\mathcal{S}^k(\mathbb{R}^d)$ denotes the space of k times continuously differentiable functions of superalgebraic decay in all derivatives up to order k ,

$$\sup_{\mathbf{z} \in \mathbb{R}^d} |\mathbf{z}^\alpha \partial^\beta \phi(\mathbf{z})| < \infty, \quad \phi \in \mathcal{S}^k(\mathbb{R}^d), \quad \alpha, \beta \in \mathbb{N}^d, \quad |\beta| \leq k.$$

Definition 6.3 (Schwartz functions). The space of smooth functions of superalgebraic decay, $\mathcal{S}^\infty(\mathbb{R}^d)$, is called the Schwartz space of test functions. In this context, we drop the exponent and simply write $\mathcal{S}(\mathbb{R}^d)$.

Definition 6.4 (Translations). For $\mathbf{y} \in \mathbb{R}^d$, let $\tau_{\mathbf{y}}$ denote the translation by \mathbf{y} , $\tau_{\mathbf{y}}\phi(\mathbf{x}) = \phi(\mathbf{x} - \mathbf{y})$, $\mathbf{x} \in \mathbb{R}^d$, for a test function $\phi \in \mathcal{D}(\mathbb{R}^d)$. It is extended to

distributions $u \in \mathcal{D}'(\mathbb{R}^d)$ via

$$(\tau_{\mathbf{y}}u)(\phi) = u(\tau_{-\mathbf{y}}\phi).$$

Definition 6.5 (Convolution). For integrable functions $f, g : \mathbb{R}^d \rightarrow \mathbb{C}$ the convolution $f * g$ is given by

$$(f * g)(\mathbf{x}) = \int_{\mathbb{R}^d} f(\mathbf{x} - \mathbf{z})g(\mathbf{z}) \, d\mathbf{z} = \int_{\mathbb{R}^d} \tau_{\mathbf{x}}\check{f}(\mathbf{z})g(\mathbf{z}) \, d\mathbf{z} \quad \mathbf{x} \in \mathbb{R}^d,$$

where \check{f} denotes $\check{f}(\mathbf{z}) = f(-\mathbf{z})$. For $u \in \mathcal{S}'(\mathbb{R}^d)$ and $\psi \in \mathcal{S}(\mathbb{R}^d)$ the convolution $u * \psi$ is defined as

$$u * \psi(\mathbf{x}) = u(\tau_{\mathbf{x}}\check{\psi}), \quad \mathbf{x} \in \mathbb{R}^d.$$

Definition 6.6 (Singular support). Let $u \in \mathcal{D}'(\Omega)$ for $\Omega \subseteq \mathbb{R}^d$ open. A point $\mathbf{x} \in \Omega$ is in the complement of the singular support of u , denoted by $\text{sing supp } u$, if there is an open neighbourhood Ω' of \mathbf{x} in Ω such that the restriction of u to Ω' can be identified with a smooth function.

Lemma 6.7. *The Fourier transformation is an automorphism on $\mathcal{S}(\mathbb{R}^d)$. By taking adjoints, \mathcal{F} and \mathcal{F}^{-1} extend to automorphism on $\mathcal{S}'(\mathbb{R}^d)$.*

In the following, we collect statements for a family of spaces that comprises the space of compactly supported test functions, smooth functions on closed or open domains, and Schwartz functions, see [44] for a general treatment of Montel spaces and tensor products.

Let $\Omega \subseteq \mathbb{R}^d$ be open or closed. By $X(\Omega)$, we denote a space of functions defined on Ω , where $X \in \{C^\infty, \mathcal{D}, \mathcal{S}\}$.

Lemma 6.8. *For a bounded sequence $(\varphi_n)_n$ in $X(\Omega)$ that converges pointwise to a function φ ,*

$$\lim_{n \rightarrow \infty} \varphi_n(\mathbf{z}) = \varphi(\mathbf{z}), \quad \mathbf{z} \in \Omega,$$

then also $\varphi \in X(\Omega)$ and the sequence converges in the topology of $X(\Omega)$ to φ .

Proof. For all X , $X(\Omega)$ is a Montel space, that is bounded sets are precompact. In particular, every bounded sequence has a converging subsequence. To prove that $(\varphi_n)_n$ converges, let $(\psi_k)_k$ denote an arbitrary subsequence. By the Montel property, it has a converging subsequence with limit ψ . Since convergence in $X(\Omega)$ implies pointwise convergence, the limit ψ has to agree with φ . Hence, every subsequence of $(\varphi_n)_n$ has a converging subsequence with limit ψ . This implies that $(\varphi_n)_n$ itself is converging in $X(\Omega)$ to $\varphi \in X(\Omega)$. \square

Lemma 6.9. *For $\Omega_1 \subseteq \mathbb{R}^{d_1}$, $\Omega_2 \subseteq \mathbb{R}^{d_2}$, both open or closed, the completion of the algebraic tensor product*

$$X(\Omega_1) \otimes X(\Omega_2)$$

in the projective or uniform topology is given by

$$X(\Omega_1 \times \Omega_2).$$

6.2. Derivation of the generalized Crandall formula. In this section, we prove the generalized Crandall formula for zeta functions on uniformly discrete sets in Theorem 3.6.

Proof of Theorem 3.6. We first restrict ν to the half plane $\operatorname{Re}(\nu) > d + k + 1$, where k is the order of the form factor $\hat{\mathbf{1}}_L$. We rewrite the interaction in terms of a Mellin transform,

$$s_\nu(\mathbf{z}) = |\mathbf{z}|^{-\nu} = \frac{\pi^{\nu/2}}{\Gamma(\nu/2)} \int_0^\infty 2t^\nu e^{-\pi \mathbf{z}^2 t^2} \frac{dt}{t}, \quad \mathbf{z} \in \mathbb{R}^d \setminus \{\mathbf{0}\}.$$

Now, we split the integration interval at $t = 1/\lambda$ and use the integral representation of G_ν in order to obtain

$$\int_{1/\lambda}^\infty 2t^\nu e^{-\pi \mathbf{z}^2 t^2} \frac{dt}{t} = \lambda^{-\nu} G_\nu(\mathbf{z}/\lambda),$$

which decays superexponentially as $|\mathbf{z}| \rightarrow \infty$, and a second term,

$$h(\mathbf{z}) = \int_0^{1/\lambda} 2t^{\nu-1} e^{-\pi t^2 |\mathbf{z}|^2} dt,$$

a smooth and bounded function with at most polynomial growth in all derivatives. To be able to insert the Riemann splitting, we need to regularize the lattice sum with an exponentially decaying factor,

$$\begin{aligned} Z_{L,\nu}(\mathbf{y}) &= \lim_{\varepsilon \rightarrow 0} \sum'_{\mathbf{z} \in L} e^{-\pi \varepsilon^2 |\mathbf{z}|^2} \frac{e^{-2\pi i \mathbf{y} \cdot \mathbf{z}}}{|\mathbf{z}|^\nu} \\ &= \frac{\pi^{\nu/2}}{\Gamma(\nu/2)} \lim_{\varepsilon \rightarrow 0} \sum'_{\mathbf{z} \in L} e^{-\pi \varepsilon^2 |\mathbf{z}|^2} e^{-2\pi i \mathbf{y} \cdot \mathbf{z}} (\lambda^{-\nu} G_\nu(\mathbf{z}/\lambda) + h(\mathbf{z})) \\ &= \frac{\pi^{\nu/2}}{\Gamma(\nu/2)} \lambda^{-\nu} \sum'_{\mathbf{z} \in L} e^{-2\pi i \mathbf{y} \cdot \mathbf{z}} G_\nu(\mathbf{z}/\lambda) + \frac{\pi^{\nu/2}}{\Gamma(\nu/2)} \lim_{\varepsilon \rightarrow 0} F_\varepsilon(\mathbf{y}), \end{aligned}$$

with

$$F_\varepsilon(\mathbf{y}) = \sum'_{\mathbf{z} \in L} e^{-\pi \varepsilon^2 |\mathbf{z}|^2} e^{-2\pi i \mathbf{y} \cdot \mathbf{z}} h(\mathbf{z}).$$

To extend the summation over the full set L in above definition, we observe

$$h(\mathbf{0}) = \int_0^{1/\lambda} 2t^{\nu-1} dt = \frac{2}{\nu} \lambda^{-\nu},$$

so we can write

$$F_\varepsilon(\mathbf{y}) = -\frac{2}{\nu} \lambda^{-\nu} [\mathbf{0} \in L] + \sum_{\mathbf{z} \in L} e^{-\pi \varepsilon^2 |\mathbf{z}|^2} e^{-2\pi i \mathbf{y} \cdot \mathbf{z}} h(\mathbf{z}),$$

where the Iverson bracket $[\mathbf{0} \in L]$ equals 1 if L includes the origin and 0 otherwise. Thus we can write F_ε as

$$F_\varepsilon(\mathbf{y}) = -\frac{2}{\nu} \lambda^{-\nu} [\mathbf{0} \in L] + \langle e^{-\pi \varepsilon^2 |\cdot|^2} e^{-2\pi i \mathbf{y} \cdot \cdot} h, \mathbf{1}_L \rangle$$

With Lemma A.1 the distributional Fourier transform of h is an element of $\mathcal{S}^k(\mathbb{R}^d)$,

$$\hat{h}(\mathbf{k}) = \lambda^{d-\nu} G_{d-\nu}(\lambda \mathbf{k}), \quad \mathbf{k} \in \mathbb{R}^d.$$

Therefore,

$$F_\varepsilon(\mathbf{y}) = -\frac{2}{\nu}\lambda^{-\nu}[\mathbf{0} \in L] + \lambda^{d-\nu} \langle (\varepsilon^{-d} e^{-\pi|\cdot|^2/\varepsilon^2} * G_{d-\nu}(\lambda\cdot))(\cdot + \mathbf{y}), \hat{\mathbf{1}}_L \rangle$$

Above dual bracket in $\mathcal{S}(\mathbb{R}^d)$ extends to $\mathcal{S}^k(\mathbb{R}^d)$ by the assumption on ν . Furthermore, the convolution of the rescaled Gaussian and $G_{d-\nu}(\lambda\cdot)$ converges in $\mathcal{S}^k(\mathbb{R}^d)$ to $G_{d-\nu}(\lambda\cdot)$ as $\varepsilon \rightarrow 0$ since it is the convolution of a Dirac sequence in $\mathcal{S}(\mathbb{R}^d) \subseteq \mathcal{S}^k(\mathbb{R}^d)$ with an element in $\mathcal{S}^k(\mathbb{R}^d)$. Hence,

$$\begin{aligned} \lim_{\varepsilon \rightarrow 0} F_\varepsilon(\mathbf{y}) &= -\frac{2}{\nu}\lambda^{-\nu}[\mathbf{0} \in L] + \lambda^{d-\nu} \langle G_{d-\nu}(\lambda(\cdot + \mathbf{y})), \hat{\mathbf{1}}_L \rangle \\ &= -\frac{2}{\nu}\lambda^{-\nu}[\mathbf{0} \in L] + \lambda^{d-\nu} \{ \hat{\mathbf{1}}_L * G_{d-\nu}(\lambda\cdot) \}(\mathbf{y}). \end{aligned}$$

To summarize,

$$\begin{aligned} Z_{L,\nu}(\mathbf{y}) &= \frac{\pi^{\nu/2}}{\lambda^\nu \Gamma(\nu/2)} \left(\sum'_{\mathbf{z} \in L} e^{-2\pi i \mathbf{y} \cdot \mathbf{z}} G_\nu(\mathbf{z}/\lambda) - \frac{2}{\nu}[\mathbf{0} \in L] \right. \\ &\quad \left. + \lambda^d \{ \hat{\mathbf{1}}_L * G_{d-\nu}(\lambda\cdot) \}(\mathbf{y}) \right) \end{aligned}$$

With the definition of G_ν at $\mathbf{0}$, we can include the Iverson bracket in the lattice sum and obtain

$$Z_{L,\nu}(\mathbf{y}) = \frac{\pi^{\nu/2}}{\lambda^\nu \Gamma(\nu/2)} \left(\sum_{\mathbf{z} \in L} e^{-2\pi i \mathbf{y} \cdot \mathbf{z}} G_\nu(\mathbf{z}/\lambda) + \lambda^d \{ \hat{\mathbf{1}}_L * G_{d-\nu}(\lambda\cdot) \}(\mathbf{y}) \right)$$

This proves the asserted equality for $\nu \in \mathbb{C}$ with $\operatorname{Re}(\nu) > d + k + 1$. To extend equality to the complex plane and show smoothness in \mathbf{y} , we split the formula into S_1 , the sum over L , and S_2 , the convolution in Fourier space. Owing to the superexponential decay of G_ν , S_1 is a smooth function of \mathbf{y} for every $\nu \in \mathbb{C}$. Note that the potential singularity at $\nu = 0$ for $\mathbf{0} \in L$ is cancelled by the inverse gamma factor in front of the sum. The same argument shows that S_1 is an analytic function of ν for every fixed $\mathbf{y} \in \mathbb{R}^d$. With Theorem 3.9, S_2 can be written as

$$S_2 = \frac{\pi^{\nu/2}}{\lambda^{\nu-d}} \frac{2}{\Gamma(\nu/2)} \int_0^1 t^{\nu-d-1} \psi_L(t/\lambda, \mathbf{y}) dt,$$

which provides an analytic continuation of the convolution for every $\mathbf{y} \notin L^*$ and, moreover, is smooth outside L^* for any $\nu \in \mathbb{C}$. \square

6.3. Derivation of the Hadamard integral representation. Having established the generalized Crandall formula in the last section, we now prove the Hadamard integral representation for the convolution in Theorem 3.9.

Lemma 6.10. *Let L be uniformly discrete whose form factor has order k and $\operatorname{Re}(\nu) > d + k$. Then for $\mathbf{y} \in \mathbb{R}^d \setminus L^*$,*

$$(\hat{\mathbf{1}}_L * G_{d-\nu}(\lambda\cdot))(\mathbf{y}) = 2 \int_0^1 t^{\nu-d-1} \psi_L(t/\lambda, \mathbf{y}) dt,$$

with $\psi_L(\cdot, \mathbf{y}) : (0, 1] \rightarrow \mathbb{C}$ smooth and defined as

$$\psi_L(t, \mathbf{y}) = (\hat{\mathbf{1}}_L * e^{-\pi \cdot^2/t^2})(\mathbf{y}), \quad t > 0.$$

Its proof requires a few technical lemmas that we prove in Appendix A.2.

Lemma 6.11. *The sequence $(\gamma_n)_{n \in \mathbb{N}_0} \subseteq \mathcal{S}^k(\mathbb{R}^d)$ with*

$$\gamma_n(\mathbf{z}) = \frac{1}{n} \sum_{j=1}^n 2(j/n)^{\mu-1} \exp(-\pi\lambda^2 n^2/j^2 |\mathbf{z}|^2), \quad \mathbf{z} \in \mathbb{R}^d,$$

converges to $G_{-\mu}$ for every $\mu \in \mathbb{C}$ with $\operatorname{Re}(\mu) > k + 1$, $k \in \mathbb{N}_0$.

Lemma 6.12. *For $u \in \mathcal{S}'(\mathbb{R}^d)$ with $U = \mathbb{R}^d \setminus \operatorname{sing\,supp} u$, the linear operator*

$$T : \mathcal{S}(\mathbb{R}^d) \rightarrow C^\infty([0, 1] \times U), \quad \varphi \mapsto T\varphi,$$

with

$$(T\varphi)(t, \mathbf{y}) = (u * \varphi(\cdot/t))(\mathbf{y}), \quad t > 0, \quad \mathbf{y} \in U,$$

and smoothly extended to $t = 0$, is well-defined and continuous. If φ is even, then $T\varphi$ has the form

$$T\varphi(t, \mathbf{y}) = t^d \eta(t^2, \mathbf{y}), \quad t \in [0, 1], \quad \mathbf{y} \in U,$$

for $\eta \in C^\infty([0, 1] \times U)$.

Proof of Lemma 6.10. For $\mathbf{y} \in \mathbb{R}^d \setminus L^*$, the smoothness of ψ_L is a consequence of Lemma 6.12. To prove the asserted equality, we use Lemma 6.11 to write

$$G_{d-\nu}(\lambda \cdot) = \lim_{n \rightarrow \infty} \frac{1}{n} \sum_{j=1}^n 2(j/n)^{d-\nu-1} \exp(-\pi\lambda^2 n^2/j^2 |\cdot|^2),$$

with convergence in $\mathcal{S}^k(\mathbb{R}^d)$. In particular,

$$\hat{\mathbf{1}}_L * (G_{d-\nu}(\lambda \cdot))(\mathbf{y}) = \lim_{n \rightarrow \infty} \frac{1}{n} \sum_{j=1}^n 2(j/n)^{d-\nu-1} \psi_L(j/n/\lambda, \mathbf{y}).$$

The right hand side is a Riemann sum and converges to the corresponding integral,

$$\lim_{n \rightarrow \infty} \frac{1}{n} \sum_{j=1}^n 2(j/n)^{d-\nu-1} \psi_L(j/n/\lambda, \mathbf{y}) = 2 \int_0^1 t^{\nu-d-1} \psi_L(t/\lambda, \mathbf{y}) dt,$$

which proves the asserted equality. \square

We are now able to prove the main result of this subsection, the integral representation for the convolution over the full range of $\nu \in \mathbb{C}$

Proof of Theorem 3.9. Lemma 6.10 already contains a proof of the statement for $\operatorname{Re}(\nu) > d+k+1$. To cover the remaining cases, we observe that owing to Lemma 6.12 we can write ψ_L as

$$\psi_L(t, \mathbf{y}) = t^d \eta(t^2, \mathbf{y}), \quad t \in [0, 1], \quad \mathbf{y} \in \mathbb{R}^d \setminus L^*,$$

with a smooth function η . Hence,

$$\lambda^d \frac{2}{\Gamma(\nu/2)} \int_0^1 t^{\nu-d-1} \psi_L(t/\lambda, \mathbf{y}) dt = \frac{2}{\Gamma(\nu/2)} \int_0^1 \tau^{\nu/2-1} \eta(\tau/\lambda^2, \mathbf{y}) d\tau, \quad \operatorname{Re}(\nu) > 0.$$

Now, the right hand side can be extended as an entire function by the Hadamard integral. Note that the inverse gamma function removes the simple poles of the meromorphic Hadamard integral. Furthermore, since η is a smooth function in both arguments, the Hadamard integral is a smooth function of \mathbf{y} too. \square

6.4. Integral representation for corner geometry. The computation of the form factor for general point sets is in general a challenging task. For a corner $L = AN_0^d$ in d dimensions, we can however compute the form factor and its singular support L^* analytically.

Lemma 6.13. *For $\mathbb{1}_{\mathbb{N}_0}$ the form factor is $(1 - \exp(-2\pi i(\cdot - i0^+)))^{-1}$.*

Proof. For $\varepsilon > 0$ let

$$\hat{\mathbf{1}}_\varepsilon(y) = \sum_{z \in \mathbb{N}_0} e^{-2\pi i(y - i\varepsilon)z} = \frac{1}{1 - \exp(-2\pi i(y - i\varepsilon))}, \quad y \in \mathbb{R}.$$

Here, the right hand side converges weakly to $(1 - \exp(-2\pi i(\cdot - i0^+)))^{-1}$, see [25, Ch. 1, Sec. 3.6.]. Furthermore, it is readily seen that the left hand side converges weakly in $S'(\mathbb{R})$ to $\hat{\mathbf{1}}_{\mathbb{N}_0}$. \square

From the explicit expression of the form factor we can immediately conclude its singular support.

Lemma 6.14. *The singular support of $\hat{\mathbf{1}}_{\mathbb{N}_0}$ is \mathbb{Z} .*

Since the Fourier transform commutes with tensor products, we furthermore obtain:

Lemma 6.15. *For $L = AN_0^d$ the form factor reads*

$$\hat{\mathbf{1}}_L = \bigotimes_{j=1}^d \left(1 - e^{-2\pi i((A^T \cdot)_j - i0^+)}\right)^{-1}.$$

The explicit expression for the form factor allows a direct characterization of its singular support L^* .

Lemma 6.16. *Let $L = AN_0^d$ and set $L^* = \text{sing supp } \hat{\mathbf{1}}_L$. Then*

$$L^* \subseteq \{\mathbf{y} \in \mathbb{R}^d : A^T \mathbf{y} \text{ has at least one integer component}\}.$$

Proof. By Lemma 6.14, we know that $\hat{\mathbf{1}}_{\mathbb{N}_0}$ has singular support \mathbb{Z} and hence can be identified with a smooth function g on $\mathbb{R} \setminus \mathbb{Z}$. Due to the tensor representation $\hat{\mathbf{1}}_{\mathbb{N}_0^d} = (\hat{\mathbf{1}}_{\mathbb{N}_0})^{\otimes d}$, we can conclude that $\hat{\mathbf{1}}_{\mathbb{N}_0^d}$ can be identified by the smooth function $g^{\otimes d}$ on $(\mathbb{R} \setminus \mathbb{Z})^d$. Hence we find for its singular support

$$\text{sing supp } \hat{\mathbf{1}}_{\mathbb{N}_0^d} \subseteq \mathbb{R}^d \setminus (\mathbb{R} \setminus \mathbb{Z})^d = \{\mathbf{y} \in \mathbb{R}^d : \mathbf{y} \text{ has at least one integer component}\}.$$

The assertion for the general case follows after noting that $\hat{\mathbf{1}}_{AN_0^d} = \hat{\mathbf{1}}_{\mathbb{N}_0^d}(A_\Lambda^T \cdot)$. \square

Theorem 6.17. *Let $L = AN_0^d - \mathbf{x}$ with $\mathbf{x} \in \mathbb{R}^d$. Then for $t > 0$ and $\mathbf{y} \in \mathbb{R}^d$*

$$t \mapsto \psi_L(t, \mathbf{y})$$

extends to a smooth function at $t = 0$.

The proof of the theorem requires a series of lemmas. In the following, we use the Euler–Maclaurin expansion, see [2, 8].

Theorem 6.18 (Euler–Maclaurin expansion). *Let $a, b \in \mathbb{Z}$ with $a < b$, $\delta \in (0, 1]$, $\ell \in \mathbb{N}_0$. For a function $f \in C^{\ell+1}[a + \delta, b + \delta]$, the Euler–Maclaurin (EM) expansion takes the form*

$$\begin{aligned} \sum_{n=a+1}^b f(n) &= \int_{a+\delta}^{b+\delta} f(y) \, dy - \sum_{k=0}^{\ell} (-1)^k \frac{B_{k+1}(1+y-\lceil y \rceil)}{(k+1)!} f^{(k)}(y) \Big|_{y=a+\delta}^{y=b+\delta} \\ &\quad + \int_{a+\delta}^{b+\delta} (-1)^{\ell} \frac{B_{\ell+1}(1+y-\lceil y \rceil)}{(\ell+1)!} f^{(\ell+1)}(y) \, dy, \end{aligned}$$

with $\lceil y \rceil$ the smallest integer larger than or equal to y . Furthermore, B_{ℓ} denote the Bernoulli polynomials, which are defined via the recurrence relation

$$B_0(y) = 1, \quad B'_{\ell}(y) = \ell B_{\ell-1}(y), \quad \int_0^1 B_{\ell}(y) \, dy = 0, \quad \ell \geq 1.$$

Lemma 6.19. *For $\mathbf{x} \in \mathbb{R}^d$, let*

$$\langle \mathbf{x} \rangle = (1 + |\mathbf{x}|^2)^{1/2}.$$

Then for all $\mathbf{x}, \mathbf{y} \in \mathbb{R}^d$ and $w \in \mathbb{R}$,

$$\langle \mathbf{x} + \mathbf{y} \rangle^w \leq 2^{|w|/2} \langle \mathbf{x} \rangle^w \langle \mathbf{y} \rangle^{|w|}$$

Lemma 6.20. *For $u = \hat{\mathbf{1}}_{\mathbb{N}_0-x}$, $x \in \mathbb{R}$, Lemma 6.12 holds for all $y \in \mathbb{R}$.*

Proof. The singular support of $u = \hat{\mathbf{1}}_{\mathbb{N}_0-x}$ is

$$\text{sing supp } u = L^* = \mathbb{Z}$$

by Lemma 6.14. Lemma 6.12 proves the assertion for $y \in \mathbb{R} \setminus L^*$. Hence, we only need to study $y \in L^* = \mathbb{Z}$. The convolution with the form factor reads

$$(T\varphi)(t) = t \sum_{z \in \mathbb{N}_0-x} e^{-2\pi iz \cdot y} \hat{\varphi}(tz) = e^{2\pi iz \cdot x t} \sum_{z \in \mathbb{N}_0} \hat{\varphi}(t(z-x)), \quad t > 0,$$

where we have used that $e^{-2\pi iy \cdot z} = 1$ for $y \in \mathbb{Z}$ and $z \in \mathbb{N}_0$. To prove smoothness of $T\varphi$ on $[0, 1]$ we show that $T\varphi \in C^{2\ell-1}([0, 1])$ for all $\ell \in \mathbb{N}$. Owing to the equality

$$C^{\infty}([0, 1]) = \bigcap_{\ell \in \mathbb{N}} C^{2\ell-1}([0, 1])$$

it follows $T\varphi \in C^{\infty}([0, 1])$. Furthermore, we bound all derivatives by Schwartz seminorms of φ thus implying the continuity of the mapping T from $S(\mathbb{R})$ to $C^{\infty}([0, 1])$. Now, let $\ell \in \mathbb{N}$. We apply the Euler–Maclaurin expansion of order 2ℓ as stated in Theorem 6.18,

$$t \sum_{z \in \mathbb{N}_0} \hat{\varphi}(t(z-x)) = \mathcal{I}(t) + \mathcal{D}(t) + \mathcal{R}(t),$$

with integral part \mathcal{I} , differential operator part \mathcal{D} , and remainder \mathcal{R} given by

$$\begin{aligned}\mathcal{I}(t) &= t \int_{\mathbb{R}_+} \hat{\varphi}(t(z-x)) dz, \\ \mathcal{D}(t) &= \sum_{k=0}^{2\ell-1} c_k t^{k+1} \hat{\varphi}^{(k)}(-tx), \\ \mathcal{R}(t) &= \int_{\mathbb{R}_+} B_{2\ell}(z) t^{2\ell+1} \hat{\varphi}^{(2\ell)}(t(z-x)) dz,\end{aligned}$$

for $t \in (0, 1]$ with constants $c_k \in \mathbb{R}$ and $B_{2\ell}$ a continuous bounded \mathbb{Z} -periodic function. We demonstrate smoothness of the sum by showing the smoothness of its three parts. For the integral part, we find after a change of variables that

$$\mathcal{I}(t) = \int_{\mathbb{R}_+} \hat{\varphi}(z-tx) dz, \quad t \in [0, 1].$$

Now,

$$|\partial_t^n(\hat{\varphi}(z-tx))| = |x|^n |\hat{\varphi}^{(n)}(z-tx)| \leq |x|^n \|\hat{\varphi}\|_{n,1} \langle z-tx \rangle^{-1} \leq \sqrt{2} \langle x \rangle^{n+1} \|\hat{\varphi}\|_{n,1} \langle z \rangle^{-1},$$

by Lemma 6.19, where $\|\cdot\|_{k,p}$ denotes a weighted Schwartz seminorm

$$\|\psi\|_{n,p} = \sup_{z \in \mathbb{R}} |\langle z \rangle^p \psi^{(n)}(z)|, \quad \psi \in \mathcal{S}(\mathbb{R}).$$

Above estimates constitute uniform integrable bounds on all derivatives with respect to t , valid on $[0, 1]$. Hence, \mathcal{I} is a smooth function on $(0, 1]$ with finite limits of all derivatives for $t \rightarrow 0$ by the dominated convergence theorem. Consequently, \mathcal{I} is a smooth function on $[0, 1]$ with

$$|\partial_t^n \mathcal{I}(t)| \leq C_n \|\hat{\varphi}\|_{n,1},$$

for a constant $C_n > 0$ that only depends on the derivative order. Furthermore, \mathcal{D} is a smooth function on $[0, 1]$ as the composition of smooth functions. A direct computation reveals the uniform bound in terms of seminorms of $\hat{\varphi}$,

$$|\partial_t^n \mathcal{D}(t)| \leq \sum_{k=0}^{2\ell-1+n} d_k \|\hat{\varphi}\|_{k,0},$$

for constants $d_k > 0$. For the remainder \mathcal{R} we first note that a similar argument as for \mathcal{I} shows that \mathcal{R} is smooth on $(0, 1]$. We now prove that the first $2\ell - 1$ derivatives of \mathcal{R} vanish at $t = 0$. We have that

$$\begin{aligned}\partial_t^n \mathcal{R}(t) &= \sum_{m=0}^n \int_{\mathbb{R}_+} c_m B_{2\ell}(z) t^{2\ell+1-m} (tz)^{n-m} \hat{\varphi}^{(2\ell+n-m)}(t(z-x)) dz, \\ &= \sum_{m=0}^n c_m t^{2\ell-m} \int_{\mathbb{R}_+} B_{2\ell}(z/t) z^{n-m} \hat{\varphi}^{(2\ell+n-m)}(z-tx) dz,\end{aligned}$$

for $t > 0$. Using that $B_{2\ell}$ is bounded on \mathbb{R} , we can establish the bound

$$|\partial_t^n \mathcal{R}(t)| \leq \sum_{m=0}^n r_m t^{2\ell-m} \|\hat{\varphi}\|_{2\ell+n-m, n-m+1},$$

for constants $r_m > 0$. It follows

$$\lim_{t \rightarrow 0} \partial_t^n \mathcal{R}(t) = 0,$$

for $n \leq 2\ell - 1$ and hence $\mathcal{R} \in C^{2\ell-1}([0, 1])$.

To summarize, we have shown that all derivatives of $T\varphi$ on $[0, 1]$ are bounded by a sum of Schwartz seminorms of $\hat{\varphi}$. In particular, for all $n \in \mathbb{N}_0$ there exists a continuous seminorm q_n on $S(\mathbb{R})$ with

$$\sup_{t \in [0, 1]} |\partial_t^n T\varphi(t)| \leq q_n(\hat{\varphi}).$$

Since the Fourier transform is automorphism on $S(\mathbb{R})$, there is a continuous seminorm p_n with

$$\sup_{t \in [0, 1]} |\partial_t^n T\varphi(t)| \leq q_n(\hat{\varphi}) \leq p_n(\varphi),$$

hence proving the assertion. \square

Lemma 6.21. *Let $u_1, \dots, u_d \in S'(\mathbb{R})$ be tempered distributions. Fix $\mathbf{y} \in \mathbb{R}^d$ such that the mapping T_j defined as in Lemma 6.12 for u_j and y_j , $j = 1, \dots, d$, is well-defined and continuous. Then, the corresponding mapping T for the tensor product*

$$u = \bigotimes_{j=1}^d u_j$$

and \mathbf{y} is well-defined and continuous. In particular, the mapping

$$(0, 1] \rightarrow \mathbb{C}, \quad t \mapsto \left(u * \varphi(\cdot/t) \right)(\mathbf{y})$$

extends smoothly to $t = 0$ for all Schwartz functions $\varphi \in \mathcal{S}(\mathbb{R}^d)$.

Proof. We first define the related mapping $\tilde{T} : \mathcal{S}(\mathbb{R}^d) \rightarrow C^\infty((0, 1]^d)$ with

$$(\tilde{T}\varphi)(\mathbf{t}) = \left(u * \varphi(\cdot/\mathbf{t}) \right)(\mathbf{y}), \quad \varphi \in \mathcal{S}(\mathbb{R}^d), \quad \mathbf{t} \in (0, 1]^d,$$

interpreting division by the vector \mathbf{t} element-wise. Note that if φ is the tensor product of one-dimensional Schwartz functions,

$$\varphi = \bigotimes_{j=1}^d \varphi_j, \quad \varphi_j \in \mathcal{S}(\mathbb{R}),$$

the mapping \tilde{T} factorizes,

$$\tilde{T}\varphi(\mathbf{t}) = \prod_{j=1}^d T_j \varphi_j(t_j), \quad \mathbf{t} \in (0, 1]^d.$$

In particular, the right hand side is well-defined for all $\mathbf{t} \in [0, 1]^d$. Let \hat{T} denote the unique continuous linear continuation of

$$\bigotimes_{j=1}^d T_j : \bigotimes_{j=1}^d \mathcal{S}(\mathbb{R}) \rightarrow \bigotimes_{j=1}^d C^\infty([0, 1])$$

to the completion of the algebraic tensor products, see Lemma 6.9,

$$\hat{T} : \mathcal{S}(\mathbb{R}^d) \rightarrow C^\infty([0, 1]^d).$$

By construction it agrees with \tilde{T} on pure tensors and $\mathbf{t} \in (0, 1]^d$,

$$\hat{T} \bigotimes_{j=1}^d \varphi(\mathbf{t}) = \tilde{T} \bigotimes_{j=1}^d \varphi(\mathbf{t}).$$

Since linear combinations of pure tensors are dense, $\hat{T}\varphi$ provides the unique and smooth extension of $\tilde{T}\varphi$ to $C^\infty([0, 1]^d)$. To recover the formulation of Lemma 6.12, we need to change the image space of \tilde{T} from $C^\infty([0, 1]^d)$ to $C^\infty([0, 1])$. This is accomplished by concatenation with the continuous map

$$\eta : C^\infty([0, 1]^d) \rightarrow C^\infty([0, 1]),$$

with $(\eta g)(t) = g(t, \dots, t)$, $t \in [0, 1]$. Then T is given by

$$T = \hat{T} \circ \eta,$$

by construction a continuous linear mapping from $S(\mathbb{R}^d)$ to $C^\infty([0, 1])$ with

$$T\varphi(t) = [u * \varphi(\cdot/t)](\mathbf{y}),$$

for $t \in (0, 1]$. \square

Finally, we combine the definition of ψ_L with Lemma 6.15 to arrive at the following proof of Theorem 3.9.

Proof of Theorem 3.9. Recall that ψ_L is given by the formula

$$\psi_L(t, \mathbf{y}) = (\hat{\mathbf{1}}_L * e^{-\pi \cdot^2 / t^2})(\mathbf{y}).$$

Recall also that, by Lemma 6.15, for $L = \text{AN}_0^d$ the form factor reads

$$\hat{\mathbf{1}}_L = \bigotimes_{j=1}^d \left(1 - e^{-2\pi i((A^T \cdot)_j - i0^+)} \right)^{-1},$$

from which it follows that

$$\hat{\mathbf{1}}_{L-\mathbf{x}} = e^{2\pi i \mathbf{x} \cdot (\cdot)} \bigotimes_{j=1}^d \left(1 - e^{-2\pi i((A^T \cdot)_j - i0^+)} \right)^{-1}.$$

Thus,

$$\begin{aligned} \psi_{L-\mathbf{x}}(t, \mathbf{y}) &= \int_{\mathbb{R}^d} \frac{e^{2\pi i \mathbf{x} \cdot (\mathbf{y} - \boldsymbol{\xi})} \cdot e^{-\pi \boldsymbol{\xi}^2 / t^2}}{\prod_{j=1}^d (1 - e^{-2\pi i(A^T(\mathbf{y} - \boldsymbol{\xi}))_j - i0^+})} d\boldsymbol{\xi} \\ &= e^{2\pi i \mathbf{x} \cdot \mathbf{y}} \int_{\mathbb{R}^d} \frac{e^{2\pi i \mathbf{x} \cdot \boldsymbol{\xi}} \cdot e^{-\pi \boldsymbol{\xi}^2 / t^2}}{\prod_{j=1}^d (1 - e^{-2\pi i((A^T \boldsymbol{\xi})_j + (A^T \mathbf{y})_j - i0^+)})} d\boldsymbol{\xi} \\ &= e^{2\pi i \mathbf{x} \cdot \mathbf{y}} \cdot e^{-\pi t^2 \mathbf{x}^2} \int_{\mathbb{R}^d} \frac{e^{-\pi(\boldsymbol{\xi} - it^2 \mathbf{x})^2 / t^2}}{\prod_{j=1}^d (1 - e^{-2\pi i((A^T \boldsymbol{\xi})_j + (A^T \boldsymbol{\xi})_j - i0^+)})} d\boldsymbol{\xi} \\ &= e^{2\pi i \mathbf{x} \cdot \mathbf{y}} \cdot e^{-\pi t^2 \mathbf{x}^2} \int_{\mathbb{R}^d - it^2 \mathbf{x}} \frac{e^{-\pi \boldsymbol{\xi}^2 / t^2}}{\prod_{j=1}^d (1 - e^{-2\pi i((A^T \boldsymbol{\xi})_j - t \mathbf{Y}(t)_j - i0^+)})} d\boldsymbol{\xi}, \end{aligned}$$

where $\mathbf{Y}(t) = -A^T(\mathbf{y}/t + it\mathbf{x})$. It follows that

$$\psi_{L-\mathbf{x}}(t, \mathbf{y}) = e^{2\pi i \mathbf{x} \cdot \mathbf{y}} e^{-\pi t^2 \mathbf{x}^2} \frac{1}{V_\Lambda} \int_{A^T(\mathbb{R}^d - it^2 \mathbf{x})} \frac{e^{-\pi(A^{-T} \boldsymbol{\xi})^2 / t^2}}{\prod_{j=1}^d (1 - e^{-2\pi i(\xi_j - t \mathbf{Y}(t)_j - i0^+)})} d\boldsymbol{\xi}.$$

By Cauchy's theorem, assuming that $\text{Im}(\mathbf{Y}(t)_j) \geq 0$, we have that

$$\psi_{L-\mathbf{x}}(t, \mathbf{y}) = e^{2\pi i \mathbf{x} \cdot \mathbf{y}} e^{-\pi t^2 \mathbf{x}^2} \frac{1}{V_\Lambda} \int_{\mathbb{R}^d} \frac{e^{-\pi(A^{-T} \boldsymbol{\xi})^2 / t^2}}{\prod_{j=1}^d (1 - e^{-2\pi i(\xi_j - t \mathbf{Y}(t)_j - i0^+)})} d\boldsymbol{\xi},$$

which proves the asserted representation of the convolution. \square

7. NUMERICAL ALGORITHM

Let $L = \text{AN}_0^d$, $\mathbf{x} \in \mathbb{R}^d \setminus L$, $\mathbf{y} \in \mathbb{R}^d \setminus L^*$, and $\nu \in \mathbb{C}$. In this section, we describe a numerical method for evaluating the function

$$Z_{L,\nu} \left| \begin{matrix} \mathbf{x} \\ \mathbf{y} \end{matrix} \right| = \sum'_{\mathbf{z} \in L} \frac{e^{-2\pi i \mathbf{y} \cdot \mathbf{z}}}{|\mathbf{z} - \mathbf{x}|^\nu},$$

which is directly related to the set zeta function via Remark 3.3. We first observe that, by dividing the corner $L = \text{AN}_0^d$ into subsets along the planes $\{\mathbf{z} \in \mathbb{R}^d : (A^{-1}\mathbf{z})_j = (A^{-1}\mathbf{x})_j\}$, $j = 1, 2, \dots, d$, we can represent this zeta function for $\mathbf{x} \in \mathbb{R}^d \setminus L$ by a combination of corner zeta functions, each corresponding to the case when $\mathbf{x} \in \text{AR}_{\leq 0}^d \setminus L$. We then use Remark 3.3 together with Theorem 3.6, Theorem 3.7, and Theorem 3.9 to perform our calculation. Recall that the sum over \mathbf{z} appearing in the formula for $Z_{L-\mathbf{x},\nu}(\mathbf{y})$ involves the summands $G_\nu(\mathbf{z}/\lambda)$, which decay exponentially in \mathbf{z}^2 . These summands can be written in terms of the upper incomplete gamma function, for which efficient and accurate numerical codes are available (see, for example, [26]). The main difficulty is thus the evaluation of the integral $I_{L-\mathbf{x}}(\mathbf{y}) = \int_0^1 t^{\nu-d-1} \psi_{L-\mathbf{x}}(t/\lambda, \mathbf{y}) dt$ and of the function $\psi_{L-\mathbf{x}}$. The numerical evaluation of this zeta function using these formulas depends on resolution of the following three problems:

- (1) The choice of the Riemann splitting parameter λ ;
- (2) The evaluation of the function $\psi_{L-\mathbf{x}}$;
- (3) The evaluation of the singular Hadamard finite-part integral $I_{L-\mathbf{x}}(\mathbf{y})$.

7.1. Choice of the Riemann splitting parameter λ . The Riemann splitting parameter λ controls how much of the set zeta function is computed in the sum appearing in the representation given by Theorem 3.6, and how much of it is computed in the integral $I_{L-\mathbf{x}}(\mathbf{y})$. A smaller value of λ means a smaller number of terms in the sum, as well as a larger domain of integration in the integral $I_{L-\mathbf{x}}(\mathbf{y})$, and vice versa.

First, recall that

$$G_\nu(\mathbf{z}) = \frac{\Gamma(\nu/2, \pi \mathbf{z}^2)}{(\pi \mathbf{z}^2)^{\nu/2}} \sim \frac{e^{-\pi \mathbf{z}^2}}{\pi \mathbf{z}^2} \quad \text{as } |\mathbf{z}| \rightarrow \infty.$$

Thus, for each $\varepsilon > 0$, $G_\nu(\mathbf{z}/\lambda) \geq \varepsilon$ whenever

$$|\mathbf{z}| \lesssim \lambda \sqrt{\frac{\log(1/\varepsilon)}{\pi}}.$$

Letting $\sigma_1 \geq \sigma_2 \geq \dots \geq \sigma_d > 0$ denote the eigenvalues of $A^T A$, we see that the sum over $\mathbf{z} \in A[-m, m]^d \cap (L - \mathbf{x})$, where

$$m = \frac{\lambda}{\sqrt{\sigma_d}} \sqrt{\frac{\log(1/\varepsilon)}{\pi}},$$

contains all $\mathbf{z} \in L - \mathbf{x}$ for which $G_\nu(\mathbf{z}/\lambda) \gtrsim \varepsilon$.

In order to simplify the evaluation of the function $\psi_{L-\mathbf{x}}$, we require the support of the Gaussian $e^{-\pi(A^{-T}\boldsymbol{\xi})^2}$ to contain, to precision ε , at most a single element of the set $\prod_{j=1}^d (\text{Re}(\mathbf{Y}(t)_j) + \mathbb{Z}/t)$. Since $\text{Re}(\mathbf{Y}(t)_j)$ is arbitrary, this means we require

that that $e^{-\pi(A^{-T}\boldsymbol{\xi})^2} \leq \varepsilon$ for all $\boldsymbol{\xi} \in \mathbb{R}^d \setminus [-h/(2t), h/(2t)]^d$, for some $0 < h < 1$. It is easy to see that this holds whenever

$$\lambda \geq \frac{2\sqrt{\sigma_1}}{h} \sqrt{\frac{\log(1/\varepsilon)}{\pi}}.$$

In order to ensure that the support of the Gaussian is well-separated from all other elements of $\prod_{j=1}^d (\operatorname{Re}(\mathbf{Y}(t)_j) + \mathbb{Z}/t)$ besides the single element inside the cell $[-1/(2t), 1/(2t)]^d$, we choose $h = 1/2$. Note that, if we set λ equal to this lower bound, then the total number of elements in the set $A[-m, m]^d$ grows as $O((\sigma_1/\sigma_d)^{d/2}) = O(\kappa(A)^d)$, where $\kappa(A)$ is the condition number of A .

In order to minimize the cost of evaluating the sum appearing in the representation of the zeta function, we would like to make λ as small as possible, which means setting it equal to this lower bound. There is, however, a situation in which λ can be made larger, without incurring any extra cost in the evaluation of the sum. Recall that $\mathbf{x} \in A\mathbb{R}_{\leq 0}^d \setminus L$, and suppose that

$$\operatorname{dist}(\mathbf{x}, \operatorname{Conv}(L)) \geq \lambda \sqrt{\frac{\log(1/\varepsilon)}{\pi}},$$

where $\operatorname{Conv}(L) \subseteq \mathbb{R}^d$ denotes the convex hull of the set L . In this case, there will be no terms of size larger than ε appearing in the sum. Equivalently, the sum will contain no terms larger than ε , whenever

$$\lambda \leq \operatorname{dist}(\mathbf{x}, \operatorname{Conv}(L)) \sqrt{\frac{\pi}{\log(1/\varepsilon)}}.$$

In order to avoid computing the distance between \mathbf{x} and $\operatorname{Conv}(L)$, we use the fact that $\sigma_n(A^{-1}\mathbf{x})^2 \leq \operatorname{dist}(\mathbf{x}, \operatorname{Conv}(L))^2$ to arrive at the looser but simpler bound

$$\lambda \leq \sqrt{\frac{\pi\sigma_n}{\log(1/\varepsilon)}} \cdot (A^{-1}\mathbf{x})^2 \leq \operatorname{dist}(\mathbf{x}, \operatorname{Conv}(L)) \sqrt{\frac{\pi}{\log(1/\varepsilon)}}.$$

Since we would like to make λ as small as possible in order to reduce the number of terms in the sum, and since we would like λ to be large when the sum is empty in order to reduce the domain of $I_{L-\mathbf{x}}(\mathbf{y})$, we set

$$\lambda = \max\left(\frac{2}{h} \sqrt{\frac{\sigma_1 \log(1/\varepsilon)}{\pi}}, \sqrt{\frac{\pi\sigma_d}{\log(1/\varepsilon)}} \cdot (A^{-1}\mathbf{x})^2\right).$$

7.2. Evaluation of the function $\psi_{L-\mathbf{x}}$. The representation for $\psi_{L-\mathbf{x}}$ provided in Theorem 3.9 can be understood in terms of a generalization of the classical Faddeeva w function

$$w(z) = \frac{1}{\pi i} \int_{\mathbb{R}} \frac{e^{-t^2}}{t - z} dt, \quad \operatorname{Im}(z) > 0,$$

where the definition is extended to all $z \in \mathbb{C}$ by analytic continuation. Note that $\operatorname{erfc}(x) = e^{-x^2} w(ix)$, where

$$\operatorname{erfc}(x) = 1 - \frac{2}{\sqrt{\pi}} \int_0^x e^{-t^2} dt, \quad x \in \mathbb{C}.$$

Definition 7.1 (Generalized Faddeeva function). Suppose that $u \in \mathcal{D}'(\mathbb{R}^d)$ and that $G \in \mathbb{R}^{d \times d}$ is a positive definite matrix. The generalized multidimensional Faddeeva function $w: \mathbb{C}^d \rightarrow \mathbb{C}$ is defined by the formula

$$w(\mathbf{z}; u, G) = \langle \tau_{\mathbf{z}} u(\boldsymbol{\xi}), e^{-\boldsymbol{\xi}^T G^{-1} \boldsymbol{\xi}} \rangle, \quad \mathbf{z} \in \mathbb{C}^d,$$

with the translation operator $\tau_{\mathbf{z}}$ from Definition 6.4.

Note that $w(z; \frac{1}{\pi i(\cdot - i0^+)}, 1) = w(z)$. The following theorem expresses the function $\psi_{L-\mathbf{x}}$ in terms of the generalized Faddeeva function, and follows immediately from Theorem 3.9.

Theorem 7.2. *Let $L = AN_0^d$ and suppose that $\mathbf{x} \in \mathbb{R}^d$ and $\mathbf{y} \in \mathbb{R}^d$. Then, for all $t > 0$,*

$$\psi_{L-\mathbf{x}}(t, \mathbf{y}) = e^{2\pi i \mathbf{x} \cdot \mathbf{y}} e^{-\pi t^2 \mathbf{x}^2} \frac{1}{V_{\Lambda}} w(\mathbf{Y}(t); \otimes_{j=1}^d t(1 - e^{-2\pi i t(\cdot - i0^+)})^{-1}, A^T A / \pi),$$

where

$$\mathbf{Y}(t) = -A^T(\mathbf{y}/t + i\mathbf{x}).$$

In the remainder of this section, we describe a numerical algorithm for the accurate and efficient evaluation of the generalized Faddeeva function

$$w(\mathbf{z}; \otimes_{j=1}^d f(\cdot - i0^+), G),$$

where $\mathbf{z} \in \mathbb{C}^d$, $G \in \mathbb{R}^{d \times d}$ is a positive definite matrix, and $f: \mathbb{C} \setminus (\mathbb{Z}/t) \rightarrow \mathbb{C}$ is a meromorphic function with poles at the elements of \mathbb{Z}/t , each with a residue of $(2\pi i)^{-1}$, satisfying the identity $f(z \pm 1/t) = f(z)$. We assume that the support of the Gaussian $e^{-\boldsymbol{\xi}^T G^{-1} \boldsymbol{\xi}}$ is, to precision ε , contained in the set $[-1/(4t), 1/(4t)]^d$.

We proceed by forming a Cholesky decomposition $G = \mathcal{L}\mathcal{L}^T$ of the matrix G , where \mathcal{L} is the lower triangular Cholesky factor. Such a decomposition always exists, since the matrix G is positive definite. Let $U = \mathcal{L}^{-T}$, so that $G^{-1} = \mathcal{L}^{-T}\mathcal{L}^{-1} = UU^T$. We then define $\boldsymbol{\eta}(\boldsymbol{\xi}) = U^T \boldsymbol{\xi}$, and observe that $\eta_j(\boldsymbol{\xi})$ only depends on $\xi_1, \xi_2, \dots, \xi_j$. This allows us to write down the following recursive formula. Let

$$\phi(\mathbf{z}) = w(\mathbf{z}; \otimes_{j=1}^d f(\cdot - i0^+), G),$$

for $\mathbf{z} \in \mathbb{C}^d$, and let the functions $\phi^{(k)}: \mathbb{C}^d \rightarrow \mathbb{C}$, $0 \leq k \leq d-1$, be given by the formula

$$\phi^{(k)}(\mathbf{z}^{(k)}) = \int_{\mathbb{R}} e^{-\eta_{k+1}(\mathbf{z}^{(k+1)})^2} f(\xi_{k+1} - z_{k+1} - i0^+) \phi^{(k+1)}(\mathbf{z}^{(k+1)}) d\xi_{k+1},$$

when $\text{Im}(z_{k+1}) \geq 0$, and let

$$\begin{aligned} \phi^{(k)}(\mathbf{z}^{(k)}) &= \sum_{n=-\infty}^{\infty} e^{-\eta_{k+1}(\mathbf{z}^{(k)} + (n/t)\mathbf{e}_{k+1})^2} \phi^{(k+1)}(\mathbf{z}^{(k)} + (n/t)\mathbf{e}_{k+1}) \\ &\quad + \int_{\mathbb{R}} e^{-\eta_{k+1}(\mathbf{z}^{(k+1)})^2} f(\xi_{k+1} - z_{k+1} - i0^-) \phi^{(k+1)}(\mathbf{z}^{(k+1)}) d\xi_{k+1}, \end{aligned}$$

when $\text{Im}(z_{k+1}) < 0$, where $\mathbf{z}^{(k)} = (\xi_1, \xi_2, \dots, \xi_k, z_{k+1}, z_{k+2}, \dots, z_d)$, $\mathbf{z} \in \mathbb{C}^d$, \mathbf{e}_{k+1} is the $(k+1)$ th unit vector, and $\phi^{(d)}(\boldsymbol{\xi}) = 1$. We then have that $\phi^{(0)}(\mathbf{z}) = \phi(\mathbf{z})$.

Since $\phi(\mathbf{z})$ can become large when $\text{Im}(z_j) < 0$ for some $1 \leq j \leq d$, we instead compute a scaled version $\tilde{\phi}(\mathbf{z}) = e^{-\beta} \phi(\mathbf{z})$, where β is defined as follows. Let $\bar{\mathbf{z}}$ be given by the formula $\bar{z}_j = \min(\text{Im}(z_j), 0)$ for $1 \leq j \leq d$. We then define

$\beta = \sum_{j=1}^n \eta_j(\bar{\mathbf{z}})^2$. It is possible to show from Definition 7.1 that $\tilde{\phi}(\mathbf{z}) \lesssim 1$. We now observe that that $\tilde{\phi}(\mathbf{z})$ satisfies the following recursive formula. Let the functions $\tilde{\phi}^{(k)}: \mathbb{C}^d \rightarrow \mathbb{C}$, $0 \leq k \leq d-1$, be given by the formula

$$\tilde{\phi}^{(k)}(\mathbf{z}^{(k)}) = \int_{\mathbb{R}} e^{-\eta_{k+1}(\mathbf{z}^{(k+1)})^2 - \eta_{k+1}(\bar{\mathbf{z}})^2} f(\xi_{k+1} - z_{k+1} - i0^+) \tilde{\phi}^{(k+1)}(\mathbf{z}^{(k+1)}) d\xi_{k+1},$$

when $\text{Im}(z_{k+1}) \geq 0$, and let

$$\begin{aligned} \tilde{\phi}^{(k)}(\mathbf{z}^{(k)}) &= \sum_{n=-\infty}^{\infty} e^{-\eta_{k+1}(\mathbf{z}^{(k)} + (n/t)\mathbf{e}_{k+1})^2 - \eta_{k+1}(\bar{\mathbf{z}})^2} \tilde{\phi}^{(k+1)}(\mathbf{z}^{(k)} + (n/t)\mathbf{e}_{k+1}) \\ &\quad + \int_{\mathbb{R}} e^{-\eta_{k+1}(\mathbf{z}^{(k+1)})^2 - \eta_{k+1}(\bar{\mathbf{z}})^2} f(\xi_{k+1} - z_{k+1} - i0^-) \tilde{\phi}^{(k+1)}(\mathbf{z}^{(k+1)}) d\xi_{k+1}, \end{aligned}$$

when $\text{Im}(z_{k+1}) < 0$, where $\mathbf{z}^{(k)} = (\xi_1, \xi_2, \dots, \xi_k, z_{k+1}, z_{k+2}, \dots, z_d)$, $\mathbf{z} \in \mathbb{C}^d$, \mathbf{e}_{k+1} is the $(k+1)$ th unit vector, and $\tilde{\phi}^{(d)}(\boldsymbol{\xi}) = 1$. It then holds that $\tilde{\phi}^{(0)}(\mathbf{z}) = \tilde{\phi}(\mathbf{z})$.

This recursive formula can be further simplified to eliminate the infinite sum. Let $\tilde{\mathbf{z}}$ denote the single point in the set $(\mathbf{z} + \mathbb{Z}^d/t) \cap \{z \in \mathbb{C} : \text{Re}(tz) \in [-1/2, 1/2]\}^d$. Clearly, $\phi(\tilde{\mathbf{z}}) = \phi(\mathbf{z})$. Consider now the infinite sum

$$\sum_{n=-\infty}^{\infty} e^{-\eta_{k+1}(\mathbf{z}^{(k)} + (n/t)\mathbf{e}_{k+1})^2 - \eta_{k+1}(\bar{\mathbf{z}})^2}$$

which appears in this recursive formula in the case $\text{Im}(z_{k+1}) < 0$. If we assume that $\eta_{k+1}(\text{Im}(\mathbf{z}^{(k)}))^2 \lesssim \eta_{k+1}(\bar{\mathbf{z}})^2$, for $0 \leq k \leq d-1$, then we observe that

$$\left| e^{-\eta_{k+1}(\mathbf{z}^{(k)} + (n/t)\mathbf{e}_{k+1})^2 - \eta_{k+1}(\bar{\mathbf{z}})^2} \right| \lesssim \left| e^{-\eta_{k+1}(\text{Re}(\mathbf{z}^{(k)} + (n/t)\mathbf{e}_{k+1}))^2} \right|,$$

for $n \in \mathbb{Z}$. Recalling that the support of $e^{-\boldsymbol{\xi}^T G^{-1} \boldsymbol{\xi}}$ is contained in the set $[-1/(4t), 1/(4t)]^d$, to precision ε , we see that

$$\left| e^{-\sum_{j=1}^{k+1} \eta_j(\text{Re}(\tilde{\mathbf{z}}^{(k)} + (n/t)\mathbf{e}_{k+1}))^2} \right| \lesssim \varepsilon$$

for all $n \in \mathbb{Z} \setminus \{0\}$, where $\tilde{\mathbf{z}}^{(k)} = (\xi_1, \xi_2, \dots, \xi_k, \tilde{z}_{k+1}, \tilde{z}_{k+2}, \dots, \tilde{z}_d)$. This means that the final contribution of all terms in the infinite sum, besides the one corresponding to $\tilde{\mathbf{z}}^{(k)}$, to the value of $\tilde{\phi}^{(0)}(\mathbf{z})$, is less than ε in size. Since our goal is to compute $\tilde{\phi}^{(0)}(\mathbf{z})$ to precision ε , this means that these terms can be dropped from the sum. In other words,

$$\sum_{n=-\infty}^{\infty} e^{-\eta_{k+1}(\mathbf{z}^{(k)} + (n/t)\mathbf{e}_{k+1})^2 - \eta_{k+1}(\bar{\mathbf{z}})^2} \approx e^{-\eta_{k+1}(\tilde{\mathbf{z}}^{(k)})^2 - \eta_{k+1}(\bar{\mathbf{z}})^2},$$

in the sense that the neglected terms have a contribution to the value $\tilde{\phi}^{(0)}(\mathbf{z})$ of less than ε . If we now let the functions $\tilde{\phi}^{(k)}: \mathbb{C}^d \rightarrow \mathbb{C}$, $0 \leq k \leq d-1$, be given by the formula

$$\begin{aligned} \tilde{\phi}^{(k)}(\tilde{\mathbf{z}}^{(k)}) &= \int_{\mathbb{R}} e^{-\eta_{k+1}(\tilde{\mathbf{z}}^{(k+1)})^2 - \eta_{k+1}(\bar{\mathbf{z}})^2} \\ &\quad f(\xi_{k+1} - \tilde{z}_{k+1} - i0^+) \tilde{\phi}^{(k+1)}(\mathbf{z}^{(k+1)}) d\xi_{k+1}, \end{aligned}$$

when $\text{Im}(\tilde{z}_{k+1}) \geq 0$, and let

$$\begin{aligned} \tilde{\phi}^{(k)}(\tilde{\mathbf{z}}^{(k)}) &= e^{-\eta_{k+1}(\tilde{\mathbf{z}}^{(k)})^2 - \eta_{k+1}(\tilde{\mathbf{z}})^2} \tilde{\phi}^{(k+1)}(\tilde{\mathbf{z}}^{(k)}) \\ &\quad + \int_{\mathbb{R}} e^{-\eta_{k+1}(\tilde{\mathbf{z}}^{(k+1)})^2 - \eta_{k+1}(\tilde{\mathbf{z}})^2} \\ &\quad \quad f(\xi_{k+1} - \tilde{z}_{k+1} - i0^-) \tilde{\phi}^{(k+1)}(\tilde{\mathbf{z}}^{(k+1)}) d\xi_{k+1}, \end{aligned}$$

when $\text{Im}(\tilde{z}_{k+1}) < 0$, where $\tilde{\mathbf{z}}^{(k)} = (\xi_1, \xi_2, \dots, \xi_k, \tilde{z}_{k+1}, \tilde{z}_{k+2}, \dots, \tilde{z}_d)$, $\mathbf{z} \in \mathbb{C}^d$, and $\tilde{\phi}^{(d)}(\boldsymbol{\xi}) = 1$, then we have that $\tilde{\phi}^{(0)}(\tilde{\mathbf{z}}) \approx \tilde{\phi}(\mathbf{z})$ to precision ε .

One remaining issue with this formula is that, if any of the terms $\xi_1, \xi_2, \dots, \xi_k$ appearing in the vector $\tilde{\mathbf{z}}^{(k)} = (\xi_1, \xi_2, \dots, \xi_k, \tilde{z}_{k+1}, \tilde{z}_{k+2}, \dots, \tilde{z}_d)$ have a large imaginary part, then the exponential term in the integrand will be highly oscillatory. We would like to perform a change of variables on $\xi_{k+1}, \xi_{k+2}, \dots, \xi_d$ which eliminates the imaginary parts of $\xi_1, \xi_2, \dots, \xi_k$, while keeping the values of $\eta_j(\boldsymbol{\xi})$ unchanged for $j = k+1, k+2, \dots, d$. First, we observe that $UU^T = G^{-1}$, so $U^T = U^{-1}G^{-1}$. Recall that U^{-1} is upper triangular. If we let g_1, g_2, \dots, g_d denote the columns of G , then it is easy to see that $(U^T g_\ell)_j = (U^{-1}G^{-1}g_\ell)_j = 0$ for all $1 \leq \ell < j \leq d$. This means that $\eta_j(\boldsymbol{\xi} + \alpha g_\ell) = \eta_j(\boldsymbol{\xi})$ for all $1 \leq \ell < j \leq d$ and $\alpha \in \mathbb{R}$. Let

$$\Delta_k(\boldsymbol{\xi}) = -i(g_1 |g_2| \cdots |g_k) G_k^{-1} (\text{Im}(\xi_1), \text{Im}(\xi_2), \dots, \text{Im}(\xi_k))^T,$$

where G_k is the leading principal minor of G of order k . Since G is positive definite, Sylvester's criterion tells us G_k has a positive determinant for each $1 \leq k \leq d$, so $\Delta_k(\boldsymbol{\xi})$ is well-defined. Then, $\eta_j(\boldsymbol{\xi} + \Delta_k(\boldsymbol{\xi})) = \eta_j(\boldsymbol{\xi})$ for $j = k+1, k+2, \dots, d$ and $\text{Im}((\boldsymbol{\xi} + \Delta_k(\boldsymbol{\xi}))_j) = 0$ for $j = 1, 2, \dots, k$. Making the change of variables $\xi'_j = \xi_j + \Delta_k(\tilde{\mathbf{z}}^{(k)})_j$ for $j = k+1, k+2, \dots, d$, we have that $\tilde{\phi}^{(k)}(\mathbf{z} + \Delta_k(\mathbf{z})) = \tilde{\phi}^{(k)}(\mathbf{z})$, for any $\mathbf{z} \in \mathbb{C}^d$.

This leads us to the final form of the recursive formula. Let the functions $\tilde{\phi}^{(k)}: \mathbb{C}^d \rightarrow \mathbb{C}$, $0 \leq k \leq d-1$, be given by the formula

$$\begin{aligned} \tilde{\phi}^{(k)}(\tilde{\mathbf{z}}^{(k)}) &= \int_{\mathbb{R}} e^{-\eta_{k+1}(\tilde{\mathbf{z}}^{(k+1)})^2 - \eta_{k+1}(\tilde{\mathbf{z}})^2} \\ &\quad f(\xi_{k+1} - \tilde{z}_{k+1} - i0^+) \tilde{\phi}^{(k+1)}(\tilde{\mathbf{z}}^{(k+1)}) d\xi_{k+1}, \end{aligned}$$

when $\text{Im}(\tilde{z}_{k+1}) \geq 0$, and let

$$\begin{aligned} \tilde{\phi}^{(k)}(\tilde{\mathbf{z}}^{(k)}) &= e^{-\eta_{k+1}(\tilde{\mathbf{z}}^{(k)})^2 - \eta_{k+1}(\tilde{\mathbf{z}})^2} \tilde{\phi}^{(k+1)}(\tilde{\mathbf{z}}^{(k)} + \Delta_{k+1}(\tilde{\mathbf{z}}^{(k)})) \\ &\quad + \int_{\mathbb{R}} e^{-\eta_{k+1}(\tilde{\mathbf{z}}^{(k+1)})^2 - \eta_{k+1}(\tilde{\mathbf{z}})^2} \\ &\quad \quad f(\xi_{k+1} - \tilde{z}_{k+1} - i0^-) \tilde{\phi}^{(k+1)}(\tilde{\mathbf{z}}^{(k+1)}) d\xi_{k+1}, \end{aligned}$$

when $\text{Im}(\tilde{z}_{k+1}) < 0$, where $\tilde{\mathbf{z}}^{(k)} = (\xi_1, \xi_2, \dots, \xi_k, \tilde{z}_{k+1}, \tilde{z}_{k+2}, \dots, \tilde{z}_d)$, $\mathbf{z} \in \mathbb{C}^d$, and $\tilde{\phi}^{(d)}(\boldsymbol{\xi}) = 1$. Then $\tilde{\phi}^{(0)}(\tilde{\mathbf{z}}) \approx \tilde{\phi}(\mathbf{z})$ to precision ε .

In order to evaluate this recursive formula, it is necessary for us to compute the integrals

$$I_j = \int_{\mathbb{R}} e^{-\eta_j(\tilde{\mathbf{z}}^{(j)})^2 - \eta_j(\tilde{\mathbf{z}})^2} f(\xi_j - \tilde{z}_j - i0^\pm) \tilde{\phi}^{(j)}(\tilde{\mathbf{z}}^{(j)}) d\xi_j,$$

where $f(z) = t(1 - e^{-2\pi itz})^{-1}$, for $1 \leq j \leq d$. Recall that $\boldsymbol{\eta}(\boldsymbol{\xi}) = U^T \boldsymbol{\xi}$, where U is an upper triangular matrix such that $G^{-1} = UU^T$. To evaluate I_j , we first let

$\alpha_j \in \mathbb{R}$ and $\beta_j \in \mathbb{C}$ be defined by

$$\alpha_j = U_{jj} \quad \text{and} \quad \beta_j = \sum_{k=1}^{j-1} U_{kj} \xi_k,$$

so that $\eta_j(\tilde{\mathbf{z}}^{(j)}) = \alpha_j \xi_j + \beta_j$, and let $w_j = \eta_j(\tilde{\mathbf{z}}^{(j)})$. We evaluate I_j to a precision of ε . Letting $a_j = (-\beta_j - \sqrt{\log(1/\varepsilon)})/|\alpha_j|$ and $b_j = (-\beta_j + \sqrt{\log(1/\varepsilon)})/|\alpha_j|$, we thus truncate the domain of integration from \mathbb{R} to $[a_j, b_j]$. When \tilde{z}_j is well-separated from \mathbb{R} , the function $f(\xi_j - \tilde{z}_j)$ is smooth. Since we know that $\tilde{\phi}^{(j)}(\xi_{k+1}, \xi_{k+2}, \dots, \xi_{j-1}, \xi_j, \tilde{z}_{j+1}, \dots, \tilde{z}_d)$ is also a smooth function of ξ_j , we can evaluate the integral using a standard adaptive Gauss-Legendre quadrature scheme, like the one described in [13].

Note however that, while $\tilde{\phi}^{(j)}$ is smooth, it has, relative to the scale of $[a_j, b_j]$, features on the scale of $|U_{jj}/U_{jk}|$ for $k = j+1, j+2, \dots, d$, so that the finest feature is on the scale $\min_{k>j} |U_{jj}/U_{jk}|$. From [33], we know that $\min_j |U_{jj}|/\max_{i,j} |U_{ij}| \geq 1/\kappa(U)$, where $\kappa(U)$ denotes the condition number of U . Since $\kappa(U) = \sqrt{\sigma_1/\sigma_d}$, we have then that $\min_{k>j} |U_{jj}/U_{jk}| \geq \sqrt{\sigma_d/\sigma_1}$. Therefore, the cost of the adaptive Gauss-Legendre quadrature to evaluate I_j will grow in proportion to $\log(\sigma_1/\sigma_d)$.

When \tilde{z}_j is close to \mathbb{R} and $\text{Re}(\tilde{z}_j) \in [a_j, b_j]$, the integral is nearly singular and the cost of adaptive Gauss-Legendre quadrature is prohibitive. Instead, we proceed by first dividing the interval $[a_j, b_j]$ into the three subintervals $[a_j, \text{Re}(\tilde{z}_j) - \delta_j]$, $[\text{Re}(\tilde{z}_j) - \delta_j, \text{Re}(\tilde{z}_j) + \delta_j]$, and $[\text{Re}(\tilde{z}_j) + \delta_j, b_j]$, where $\delta_j > 0$. The parameter δ_j is chosen so that the function

$$\psi_j(\xi_j) = e^{(\alpha_j \xi_j + \beta_j)^2 - w_j^2} f(\xi_j - \tilde{z}_j) (\xi_j - \tilde{z}_j) \tilde{\phi}^{(j)}(\xi_{k+1}, \xi_{k+2}, \dots, \xi_{j-1}, \xi_j, \tilde{z}_{j+1}, \dots, \tilde{z}_d),$$

which is analytic in a neighborhood of $\text{Re}(\tilde{z}_j)$, can be approximated to precision ε on the interval $[\text{Re}(\tilde{z}_j) - \delta_j, \text{Re}(\tilde{z}_j) + \delta_j]$ by a N th-order Chebyshev interpolant, with, for example, $N = 20$. Since the function ψ_j has features on the scale of $\min_{k>j} |U_{jj}/U_{jk}|$, δ_j must be chosen in proportion to these features, as, for example, $\delta_j = (1/6) \cdot (b_j - a_j) \min_{k>j} |U_{jj}/U_{jk}|$. As discussed in [40], the fact that ψ_j is accurately approximated by its N th order Chebyshev interpolant means that, in practice, ψ_j can be approximated uniformly to precision ε by a monomial expansion, where the coefficients of the monomial expansion are computed by solving a Vandermonde system using a backward stable solver. Once the approximation

$$\sum_{n=0}^N a_n (\xi_j - \text{Re}(\tilde{z}_j))^n \approx \psi_j(\xi_j),$$

has been computed, the integral

$$\int_{\text{Re}(\tilde{z}_j) - \delta_j}^{\text{Re}(\tilde{z}_j) + \delta_j} \frac{\psi_j(\xi_j)}{\xi_j - \tilde{z}_j - i0^\pm} d\xi_j$$

is evaluated from the moments

$$\int_{\text{Re}(\tilde{z}_j) - \delta_j}^{\text{Re}(\tilde{z}_j) + \delta_j} \frac{(\xi_j - \text{Re}(\tilde{z}_j))^n}{\xi_j - \tilde{z}_j - i0^\pm} d\xi_j,$$

which are computed analytically using well-known recurrence relations (see, for example [30]). When $\text{Re}(\tilde{z}_j) = 0$, the correct branch corresponding to either $i0^+$ or $i0^-$ is selected by rotating the branch cut analytically. The integrals over the intervals $[a_j, \text{Re}(\tilde{z}_j) - \delta_j]$ and $[\text{Re}(\tilde{z}_j) + \delta_j, b_j]$, when these intervals are not empty, are evaluated quickly and accurately by adaptive Gauss-Legendre quadrature, since away from

$\operatorname{Re}(\tilde{z}_j)$ the integrand is smooth. Finally, we observe that, when $\min_{k>j} |U_{jj}/U_{jk}| \leq 1$, no fine-scale features are present, and adaptive Gauss-Legendre quadrature can be replaced with quadratures of fixed orders for greater efficiency.

We observe that the integrand appearing in the formula for I_d involves only the function f , and so has no possibility of fine-scale features. This fact, combined with the availability of highly optimized numerical codes for evaluating the classical Faddeeva w function, can be leveraged to dramatically accelerate the evaluation of I_d . Recalling that $f: \mathbb{C} \setminus (\mathbb{Z}/t) \rightarrow \mathbb{C}$ is meromorphic with residue $(2\pi i)^{-1}$ at the elements of \mathbb{Z}/t , we define the function

$$\Phi_d(\xi_d) = f(\xi_d - \tilde{z}_d) - \frac{1}{2\pi i} \sum_{j=-n}^n \frac{1}{\xi_d - \tilde{z}_d - j/t},$$

which is analytic on the set $\mathbb{C} \setminus (\{j \in \mathbb{Z} : |j| > n\}/t)$. Next, we approximate Φ_d on the interval $[a_d, b_d]$ by using Cauchy's theorem combined with the trapezoidal rule. Letting $r = b_d - a_d$, we set $\zeta_j = (a_d + b_d)/2 + r e^{(2\pi j/m + \delta)i}$ and $\delta \zeta_j = (2\pi i/m) r e^{(2\pi j/m + \delta)i}$, for $j = 1, 2, \dots, m$, where $\delta \in \mathbb{R}$ is chosen so that none of the points ζ_j coincide with \tilde{z}_j . We then have that

$$\Phi_d(\xi_d) \approx \sum_{j=1}^m \frac{\Phi_d(\zeta_j)}{\xi_d - \zeta_j} \delta \zeta_j.$$

Combining these two formulas,

$$\begin{aligned} I_d \approx & \sum_{j=1}^m \Phi_d(\zeta_j) \delta \zeta_j \int_{\mathbb{R}} \frac{e^{-\eta_d(\tilde{z}^{(d)})^2 - \eta_d(\tilde{z})^2}}{\xi_d - \zeta_j} d\xi_d \\ & + \frac{1}{2\pi i} \sum_{j=-n}^n \int_{\mathbb{R}} \frac{e^{-\eta_d(\tilde{z}^{(d)})^2 - \eta_d(\tilde{z})^2}}{\xi_d - \tilde{z}_d - j/t} d\xi_d. \end{aligned}$$

The integrals appearing in this formula can be expressed in terms of the classical Faddeeva w function, which can be evaluated rapidly using, for example, the highly optimized implementation provided in [32]. In practice, we find $n = 6$ and $m = 18$ sufficient to obtain full machine precision accuracy for the function $f(z) = t(1 - e^{-2\pi itz})^{-1}$.

7.3. Evaluation of the singular Hadamard finite-part integral. The final step in evaluating the set zeta function for the corner is the evaluation of the Hadamard finite part integral

$$\oint_0^{1/\lambda} t^{\nu-d-1} \psi_{L-\mathbf{x}}(t, \mathbf{y}) dt.$$

We proceed by splitting this integral into two parts,

$$\oint_0^c t^{\nu-d-1} \psi_{L-\mathbf{x}}(t, \mathbf{y}) dt + \int_c^{1/\lambda} t^{\nu-d-1} \psi_{L-\mathbf{x}}(t, \mathbf{y}) dt.$$

In order to evaluate this first integral, we form the power series approximation

$$\psi_{L-\mathbf{x}}(t, \mathbf{y}) \approx \sum_{j=0}^m a_j (t/c)^j,$$

so that

$$\int_0^c t^{\nu-d-1} \psi_{L-\mathbf{x}}(t, \mathbf{y}) dt \approx c^{\nu-d} \sum_{j=0}^m \frac{a_j}{\nu-d+j},$$

where we compute the coefficients a_j , $0 \leq j \leq m$, by the formula

$$a_j = \frac{1}{2\pi} \int_0^{2\pi} \psi_{L-\mathbf{x}}(ce^{i\theta}, \mathbf{y}) e^{-ij\theta} d\theta \approx \frac{1}{m} \sum_{k=0}^{m-1} \psi_{L-\mathbf{x}}(ce^{2\pi ik/m}, \mathbf{y}) e^{-2\pi ijk/m}.$$

One problem with this formulation, however, is that $\psi_{L-\mathbf{x}}(t, \mathbf{y})$ can become extremely large for complex values of t , resulting in a large cancellation error. Recall that

$$\psi_{L-\mathbf{x}}(t, \mathbf{y}) = e^{2\pi i \mathbf{x} \cdot \mathbf{y}} e^{-\pi t^2 \mathbf{x}^2} \frac{1}{V_\Lambda} w(\mathbf{Y}(t); \otimes_{j=1}^d t(1 - e^{-2\pi it(\cdot - i0^+)})^{-1}, A^T A/\pi)$$

and

$$\mathbf{Y}(t) = -A^T(\mathbf{y}/t + i\mathbf{x}).$$

In the previous section, we defined

$$\phi(\mathbf{Y}(t)) = w(\mathbf{Y}(t); \otimes_{j=1}^d t(1 - e^{-2\pi it(\cdot - i0^+)})^{-1}, A^T A/\pi),$$

as well as a scaled version $\tilde{\phi}(\mathbf{Y}(t)) = e^{-\beta} \phi(\mathbf{Y}(t))$, so that $\tilde{\phi}(\mathbf{Y}(t)) \lesssim 1$. When $t > 0$ is real, it is generally the case that $e^{-\pi t^2 \mathbf{x}^2 + \beta} \lesssim 1$, since $\pi t^2 \mathbf{x}^2 = \pi(A^{-T} \text{Im}(\mathbf{Y}(t)))^2$, however, for complex t , this relationship no longer holds. In order to evaluate the coefficients a_j , $0 \leq j \leq m$, stably, we must ensure that the integrand remains small.

To proceed, we will first need to modify the definitions of the number $\tilde{\mathbf{z}}$ and the functions $\tilde{\phi}^{(k)}: \mathbb{C}^d \rightarrow \mathbb{C}$, $0 \leq k \leq d-1$, introduced in the previous section. Suppose that $\gamma \in \{0, 1\}^d$, and let $\tilde{\mathbf{z}}_\gamma = \tilde{\mathbf{z}} \odot \gamma$, where \odot represents componentwise multiplication, with $\tilde{\mathbf{z}}$ defined as before. Let $\beta_\gamma = \sum_{j=1}^n \eta_j(\tilde{\mathbf{z}}_\gamma)$. Next, let the functions $\tilde{\phi}_\gamma^{(k)}: \mathbb{C}^d \rightarrow \mathbb{C}$, $0 \leq k \leq d-1$, be defined by the formula

$$\begin{aligned} \tilde{\phi}_\gamma^{(k)}(\tilde{\mathbf{z}}^{(k)}) &= \int_{a_{k+1}}^{b_{k+1}} e^{-\eta_{k+1}(\tilde{\mathbf{z}}^{(k+1)})^2 - \eta_{k+1}(\tilde{\mathbf{z}}_\gamma)^2} \\ &\quad f(\xi_{k+1} - \tilde{z}_{k+1} - i0^+) \tilde{\phi}^{(k+1)}(\tilde{\mathbf{z}}^{(k+1)}) d\xi_{k+1}, \end{aligned}$$

when either $\text{Im}(\tilde{z}_{k+1}) \geq 0$ or $\gamma_{k+1} = 0$, and let

$$\begin{aligned} \tilde{\phi}_\gamma^{(k)}(\tilde{\mathbf{z}}^{(k)}) &= e^{-\eta_{k+1}(\tilde{\mathbf{z}}^{(k)})^2 - \eta_{k+1}(\tilde{\mathbf{z}}_\gamma)^2} \tilde{\phi}^{(k+1)}(\tilde{\mathbf{z}}^{(k)} + \Delta_{k+1}(\tilde{\mathbf{z}}^{(k)})) \\ &\quad + \int_{a_{k+1}}^{b_{k+1}} e^{-\eta_{k+1}(\tilde{\mathbf{z}}^{(k+1)})^2 - \eta_{k+1}(\tilde{\mathbf{z}}_\gamma)^2} \\ &\quad f(\xi_{k+1} - \tilde{z}_{k+1} - i0^-) \tilde{\phi}^{(k+1)}(\tilde{\mathbf{z}}^{(k+1)}) d\xi_{k+1}, \end{aligned}$$

when $\text{Im}(z_{k+1}) < 0$ and $\gamma_{k+1} = 1$, where $\tilde{\mathbf{z}}^{(k)} = (\xi_1, \xi_2, \dots, \xi_k, \tilde{z}_{k+1}, \tilde{z}_{k+2}, \dots, \tilde{z}_d)$, $\mathbf{z} \in \mathbb{C}^d$, and $\tilde{\phi}_\gamma^{(d)}(\boldsymbol{\xi}) = 1$. Suppose that, for each j for which $\gamma_j = 0$, we have that $|\text{Im}(z_j)| \leq H_1$, where the set on which $e^{\boldsymbol{\xi}^T G^{-1} \boldsymbol{\xi}} \leq 1$ is contained in $[-H_1, H_1]^d$, and that $|\text{Re}(z_j)| \geq \bar{H}_\varepsilon$, where the support of $e^{-\boldsymbol{\xi}^T G^{-1} \boldsymbol{\xi}}$ to precision ε is contained in $[-\bar{H}_\varepsilon, \bar{H}_\varepsilon]^d$. Then, it is easy to see that $\tilde{\phi}_\gamma^{(0)}(\tilde{\mathbf{z}}) \approx \tilde{\phi}^{(0)}(\tilde{\mathbf{z}})$, to precision ε .

Consider now $\tilde{\mathbf{z}} = \mathbf{Y}(t)$, where $A^T \mathbf{y} \in [-1/2, 1/2]^d$. Let $\gamma \in \{0, 1\}^d$ and suppose that $\gamma_j = 1$ whenever $(A^T \mathbf{y})_j = 0$ and $\gamma_j = 0$ otherwise, for $1 \leq j \leq d$. Then, for sufficiently small $t > 0$, we have that $\tilde{\phi}_\gamma^{(0)}(\mathbf{Y}(t)) \approx \tilde{\phi}^{(0)}(\mathbf{Y}(t))$, to precision ε . Notice

that $\phi^{(0)}(\mathbf{Y}(ce^{i\theta}))$ can become very large for $0 \leq \theta < 2\pi$, even for small values of $c > 0$, while $\phi_{\boldsymbol{\gamma}}^{(0)}(\mathbf{Y}(ce^{i\theta})) = e^{\beta_{\boldsymbol{\gamma}}}\tilde{\phi}_{\boldsymbol{\gamma}}^{(0)}(\mathbf{Y}(ce^{i\theta})) \lesssim 1$ for all $0 \leq \theta < 2\pi$, provided that $c > 0$ is sufficiently small.

The parameter $c > 0$ can be chosen as follows. First, letting $\sigma_1 \geq \sigma_2 \geq \dots \geq \sigma_d > 0$ denote the eigenvalues of $A^T A$, it is easy to see that the support of $e^{-\pi(A^{-T}\boldsymbol{\xi})^2}$ is, to precision ε , contained in $[-\bar{H}_\varepsilon, \bar{H}_\varepsilon]^d$ where $\bar{H}_\varepsilon = \sqrt{\sigma_1 \log(1/\varepsilon)/\pi}$. Likewise, we see that $e^{\pi(A^{-T}\boldsymbol{\xi})^2} \leq 1$ on the set $[-H_1, H_1]^d$ where $H_1 = \sqrt{\sigma_d/\pi}$. In order to use $\tilde{\phi}_{\boldsymbol{\gamma}}^{(0)}(\mathbf{Y}(ce^{i\theta}))$ to compute the coefficients of our power series approximation, this function must be periodic and smooth in θ , which will be the case only if $(\mathbf{Y}(ce^{i\theta}))_j$ avoids the branch cut $[a_j, b_j]$, for all $1 \leq j \leq d$ for which $\gamma_j = 0$. We now observe that $|(\mathbf{Y}(ce^{i\theta}))_j| \geq |(A^T \mathbf{y})_j|/c - c|(A^T \mathbf{x})_j|$, for all $1 \leq j \leq d$, provided that c is sufficiently small. Therefore, the branch cuts $[a_j, b_j]$ are avoided by $(\mathbf{Y}(ce^{i\theta}))_j$, for all $1 \leq j \leq d$ for which $\gamma_j = 0$, over all $0 \leq \theta < 2\pi$, provided that $|(A^T \mathbf{y})_j|/c - c|(A^T \mathbf{x})_j| \geq \bar{H}_\varepsilon$, for all $1 \leq j \leq d$ for which $\gamma_j = 0$. In order for $\phi_{\boldsymbol{\gamma}}^{(0)}(\mathbf{Y}(ce^{i\theta}))$ to remain small for $0 \leq \theta < 2\pi$, we also require that $c|(A^T \mathbf{x})_j| \leq H_1$, for all $1 \leq j \leq d$ for which $\gamma_j = 1$. Finally, to ensure both that $c|(A^T \mathbf{x})_j| \leq H_1$ for all $1 \leq j \leq d$ and that $e^{-\pi t^2 \mathbf{x}^2}$ is small, we require that $c \leq 1/(|\mathbf{x}|\sqrt{\pi})$. The largest value of $c \leq 1/\lambda$ which satisfies these conditions is then selected.

Note that, when t is complex, the special scheme described in the previous section for accelerating the evaluation of the inner-most integral using the classical Faddeeva function, cannot be used. Once the Hadamard finite part integral over $[0, c]$ is evaluated, the remaining integral over the interval $[c, 1/\lambda]$ is then evaluated using a standard adaptive integration scheme.

8. NUMERICAL EXPERIMENTS

In this section, we present several numerical experiments demonstrating the accuracy and efficiency of our algorithm. We check the accuracy of the algorithm using known formulas for specific infinite discrete sets in Section 8.1 and test the algorithm on subsets of general lattices in Section 8.2.

8.1. Comparison to known formulas. There exist known analytical formulas for zeta functions over certain infinite discrete sets. In this section, we evaluate the accuracy of our algorithm by evaluating these zeta functions, and comparing our

results with these formulas. We consider the sums

$$\begin{aligned}
S_1 &= \sum_{m,n \in \mathbb{N}} (m^2 + n^2)^{-\nu/2}, \\
S_2 &= \sum_{m,n \in \mathbb{N}} (m^2 + n^2)^{-\nu/2} (-1)^{m+n}, \\
S_3 &= \sum_{m,n \in \mathbb{N}} (m^2 + n^2)^{-\nu/2} (-1)^{n-1}, \\
S_4 &= \sum_{k,\ell \in 2\mathbb{N}-1} (k^2 + \ell^2)^{-\nu/2}, \\
S_5 &= \sum_{\substack{m \in \mathbb{N} \\ p \in 2\mathbb{N}}} (m^2 + p^2)^{-\nu/2}, \\
S_6 &= \sum_{k_1, k_2, k_3, k_4 \in 2\mathbb{N}-1} (k_1^2 + k_2^2 + k_3^2 + k_4^2)^{-\nu/2}, \\
S_7 &= 4 \sum_{\ell, m, n \in \mathbb{N}} \left((\ell - \frac{1}{2})^2 + m^2 + n^2 \right)^{-\nu/2} (-1)^m.
\end{aligned}$$

Analytical formulas expressing these sums in terms of the Riemann zeta function $\zeta(s)$ and the functions

$$\begin{aligned}
\beta(s) &= \sum_{n=0}^{\infty} (-1)^n (2n+1)^{-s}, \\
A(s) &= \sum_{n=0}^{\infty} (-1)^n (4n+1)^{-s},
\end{aligned}$$

and

$$B(s) = \sum_{n=1}^{\infty} (-1)^{n+1} (4n-1)^{-s},$$

are presented by Glasser in [27, 28] with corrections by Zucker in [46]. We summarize these results in Table 1.

The sums S_1, S_2, \dots, S_7 can be easily expressed as evaluations of $Z_{A\mathbb{N}_0, \nu} \left| \frac{\mathbf{x}}{\mathbf{y}} \right|$, for the values of A , \mathbf{x} , and \mathbf{y} provided in Table 2.

We evaluate our algorithm by comparing our numerically computed results with the formulas provided in Table 1, where the formulas are evaluated using Mathematica to 200 digits of precision. We report $E = \min(E_{\text{abs}}, E_{\text{rel}})$, where E_{abs} is the absolute error and E_{rel} is the relative error, over a range of ν from $-2 + 10^{-4}$ to $10 + 10^{-4}$, with values sampled in increments of $1/80$. The results are presented in Fig. 3. We do not report the timings, however, the entire experiment was carried out in less than 10 minutes on a laptop with 16 GB of RAM and an Intel 8th Gen. Core i7-8550U CPU.

8.2. Subsets of general lattices. In this section, we apply our algorithm to subsets of general lattices of the form $\Lambda = AZ^d$. In order to provide a concise description of the lattice matrix A , we use the following crystallographic conventions. Suppose that $d = 3$, and let \mathbf{a} , \mathbf{b} , and \mathbf{c} denote the columns of A . Let $a = |\mathbf{a}|$, $b = |\mathbf{b}|$, and $c = |\mathbf{c}|$, and let α denote the angle between \mathbf{b} and \mathbf{c} , β denote the

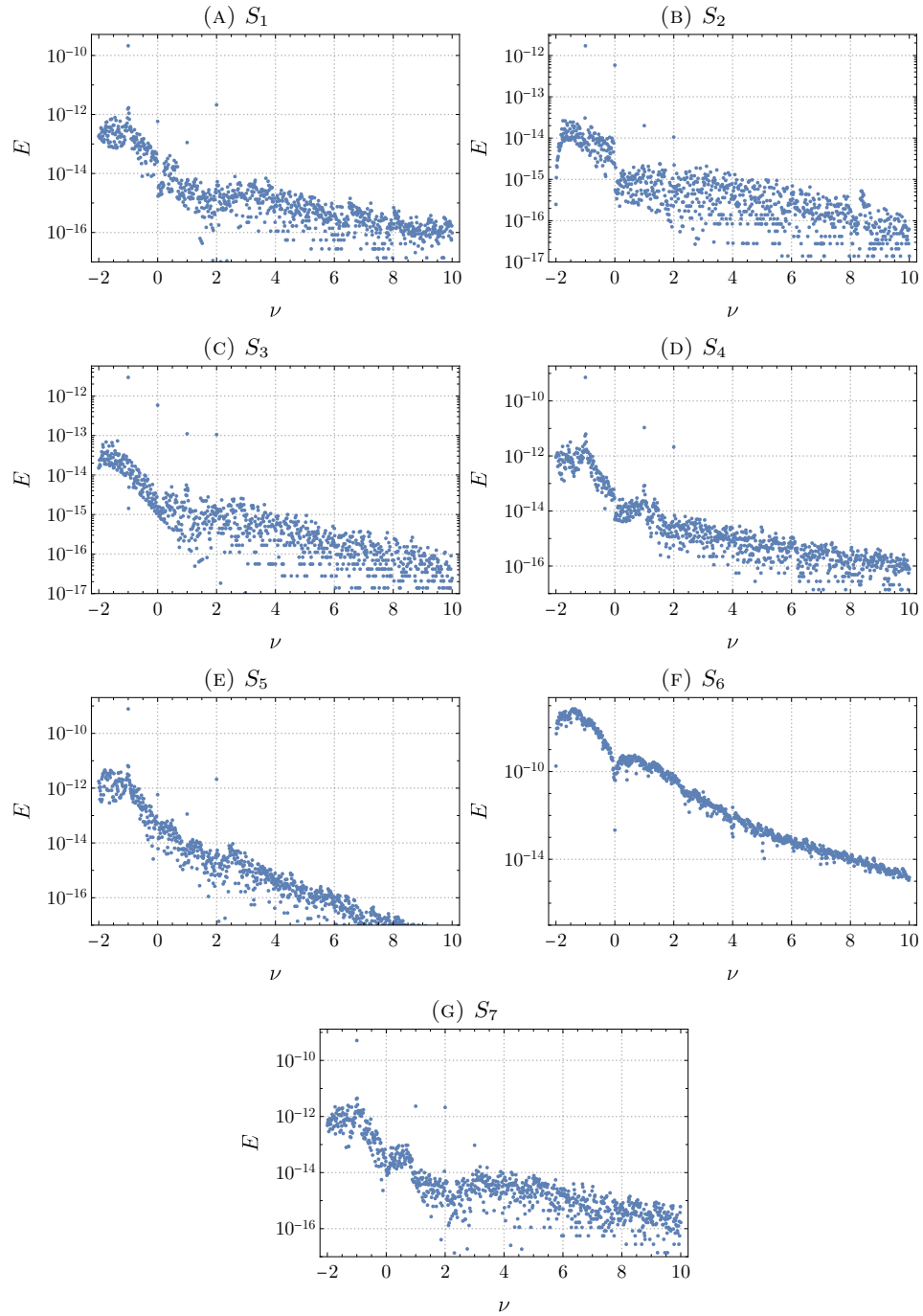


FIGURE 3. The error $E = \min(E_{\text{abs}}, E_{\text{rel}})$ of our algorithm for certain lattice sums.

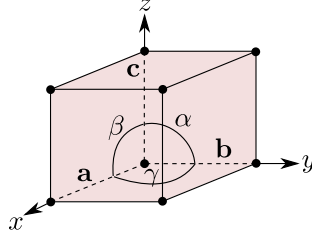
Sum	Value
S_1	$\zeta(\frac{\nu}{2})\beta(\frac{\nu}{2}) - \zeta(\nu)$
S_2	$(2^{1-\nu/2} - 1)\zeta(\frac{\nu}{2})\beta(\frac{\nu}{2}) + (1 - 2^{1-\nu})\zeta(\nu)$
S_3	$(2^{-\nu/2} - 2^{1-\nu})\zeta(\frac{\nu}{2})\beta(\frac{\nu}{2}) + 2^{-\nu}\zeta(\nu)$
S_4	$2^{-\nu/2}(1 - 2^{-\nu/2})\beta(\frac{\nu}{2})\zeta(\frac{\nu}{2})$
S_5	$\frac{1}{2}(1 - 2^{-\nu/2} + 2^{1-\nu})\zeta(\frac{\nu}{2})\beta(\frac{\nu}{2}) - \frac{1}{2}(1 + 2^{-\nu})\zeta(\nu)$
S_6	$2^{-\nu}(1 - 2^{-\nu/2})(1 - 2^{1-\nu/2})\zeta(\frac{\nu}{2})\zeta(\frac{\nu}{2} - 1)$
S_7	$2^\nu(\beta(\nu - 1) - A(\frac{\nu}{2})^2 + B(\frac{\nu}{2})^2 - (1 - 2^{-\nu/2})\zeta(\frac{\nu}{2})\beta(\frac{\nu}{2}) + (1 - 2^{-\nu})\zeta(\nu))$

TABLE 1. Analytical formulas provided in [27, 28, 46] expressing certain lattice sums in terms of the functions $\zeta(s)$, $\beta(s)$, $A(s)$, and $B(s)$.

Sum	\mathbf{x}^T	\mathbf{y}^T	A
S_1	$(-1, -1)$	$(0, 0)$	$\begin{pmatrix} 1 & 0 \\ 0 & 1 \end{pmatrix}$
S_2	$(-1, -1)$	$(\frac{1}{2}, \frac{1}{2})$	$\begin{pmatrix} 1 & 0 \\ 0 & 1 \end{pmatrix}$
S_3	$(-1, -1)$	$(\frac{1}{2}, 0)$	$\begin{pmatrix} 1 & 0 \\ 0 & 1 \end{pmatrix}$
S_4	$(-1, -1)$	$(0, 0)$	$\begin{pmatrix} 2 & 0 \\ 0 & 2 \end{pmatrix}$
S_5	$(-1, -2)$	$(0, 0)$	$\begin{pmatrix} 1 & 0 \\ 0 & 2 \end{pmatrix}$
S_6	$(-2, -2, -2, -2)$	$(0, 0)$	$\begin{pmatrix} 1 & 0 & 0 & 0 \\ 0 & 1 & 0 & 0 \\ 0 & 0 & 1 & 0 \\ 0 & 0 & 0 & 1 \end{pmatrix}$
S_7	$(-\frac{1}{2}, -1, -1)$	$(0, \frac{1}{2}, 0)$	$\begin{pmatrix} 1 & 0 & 0 \\ 0 & 1 & 0 \\ 0 & 0 & 1 \end{pmatrix}$

TABLE 2. The values of \mathbf{x} , \mathbf{y} , and A for expressing certain lattice sums in terms of the function $Z_{\text{AN}_0, \nu} \left| \frac{\mathbf{x}}{\mathbf{y}} \right|$.

angle between \mathbf{a} and \mathbf{c} , and γ denote the angle between \mathbf{a} and \mathbf{b} (see Fig. 4). The parameters a , b , c , α , β , γ are known as the lattice parameters. For $d = 2$, the lattice is summarized by lattice parameters a , b , and γ , while for $d = 1$, the lattice is summarized by just a . In this section, we consider the zeta function over the finite sublattice $L = \Lambda \cap (A \prod_{j=1}^d [0, m])$, where m is a nonnegative even integer. The lattice matrices considered in this section are shown in Table 3.

FIGURE 4. The lattice parameters indicated on the unit cell E_Λ .

The experiments were performed on Erlangen National High Performance Computing Center (NHR@FAU), on the Fritz parallel CPU cluster. Each individual zeta function evaluation was performed using a single computational thread. We implemented our algorithm using a combination of Fortran 77 and Fortran 90, and compiled it using the `gfortran` compiler, version 8.5.0, with the `-O3` and `-march=native` flags.

We first tested our algorithm over a wide range of parameters \mathbf{x} and \mathbf{y} . Letting $S = \prod_{j=1}^d \{-m/2, 0, m/2\} + \prod_{j=1}^d \{-\frac{1}{2}, 0, \frac{1}{2}\}$, we evaluated the zeta function at the points $\mathbf{x} \in AS$. Similarly, we chose $\mathbf{y} \in A^{-T} \prod_{j=1}^d \{0, 1/3, 2/3\}$. The results of our algorithm are shown in Table 4 for $\nu = d + 0.1$, in which we use the following notation.

- N : The total numbers of points in the lattice: $(m + 1)^d$.
- E_{\max} : The maximum, over all points \mathbf{x} and \mathbf{y} , of the minimum of the absolute error E_{abs} and relative error E_{rel} , $E_{\max} = \max_{\mathbf{x}, \mathbf{y}} \min(E_{\text{abs}}, E_{\text{rel}})$.
- t_{\min}, t_{\max} : The minimum and maximum CPU time required for the evaluation of the set zeta function using our algorithm, over all points \mathbf{x} and \mathbf{y} .
- t_{avg} : The average CPU time required for the evaluation of the set zeta function using our algorithm, over all points \mathbf{x} and \mathbf{y} .
- t_{naive} : The maximum CPU time required for the evaluation of the set zeta function using our naive summation, over all points \mathbf{x} and \mathbf{y} .

Matrix	d	a	b	c	α	β	γ
A_1	$d = 1$	1.1	-	-	-	-	-
A_2	$d = 2$	1.1	1.2	-	-	-	$2\pi/3$
A_3	$d = 2$	1.1	1.2	-	-	-	$\pi/2$
A_4	$d = 3$	1.1	1.2	1.3	$\pi/2$	$\pi/2$	$2\pi/3$
A_5	$d = 3$	1.1	1.2	1.3	$\pi/2$	$\pi/2$	$\pi/2$

TABLE 3. The lattice matrices considered in our experiments.

To show the effect of varying ν , we also report the error $E = \min(E_{\text{abs}}, E_{\text{rel}})$, evaluated at $\mathbf{x} = A(-\frac{1}{2})_{j=1}^d$ and $\mathbf{y} = 0$, for ν from $-5 + 10^{-4}$ to $5 + 10^{-4}$, with values sampled in increments of $1/80$. For $d = 1$, we consider the lattice L with $m = 10^4$ and lattice matrix A_1 ; for $d = 2$, we consider the lattice L with $m = 10^2$ and lattice matrix A_2 ; and for $d = 3$, we consider the lattice L with $m = 22$ and lattice matrix A_3 . The results are shown in Fig. 5.

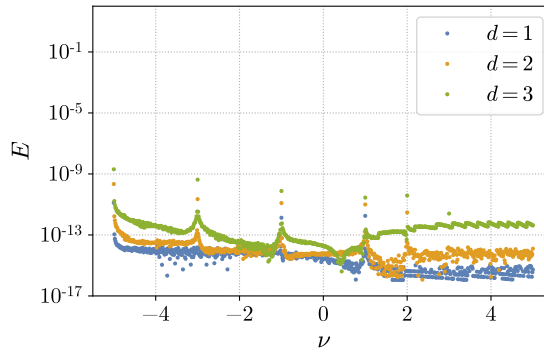
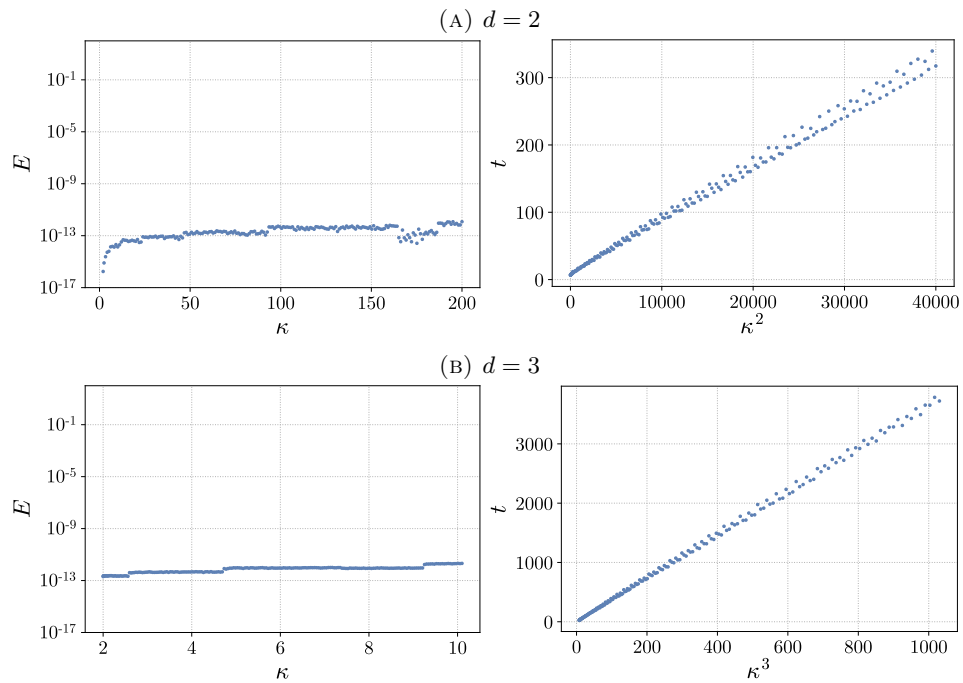
Matrix	m	N	E_{\max}	$t_{\min}-t_{\max}$	t_{avg}	t_{naive}
A_1	$1.00 \cdot 10^2$	$1.00 \cdot 10^2$	$5.79 \cdot 10^{-15}$	$1.49 \cdot 10^{-2} - 6.04 \cdot 10^{-2}$	$2.96 \cdot 10^{-2}$	$1.02 \cdot 10^{-3}$
	$1.00 \cdot 10^4$	$1.00 \cdot 10^4$	$2.88 \cdot 10^{-15}$	$1.48 \cdot 10^{-2} - 5.99 \cdot 10^{-2}$	$2.89 \cdot 10^{-2}$	$3.20 \cdot 10^{-2}$
	$1.00 \cdot 10^6$	$1.00 \cdot 10^6$	$2.52 \cdot 10^{-15}$	$1.01 \cdot 10^{-2} - 4.11 \cdot 10^{-2}$	$1.98 \cdot 10^{-2}$	$2.15 \cdot 10^0$
	$1.00 \cdot 10^8$	$1.00 \cdot 10^8$	$2.49 \cdot 10^{-15}$	$1.01 \cdot 10^{-2} - 4.10 \cdot 10^{-2}$	$1.98 \cdot 10^{-2}$	$2.15 \cdot 10^2$
	$1.00 \cdot 10^{10}$	$1.00 \cdot 10^{10}$	–	$9.83 \cdot 10^{-3} - 4.25 \cdot 10^{-2}$	$2.03 \cdot 10^{-2}$	–
	$1.00 \cdot 10^{14}$	$1.00 \cdot 10^{14}$	–	$9.83 \cdot 10^{-3} - 4.06 \cdot 10^{-2}$	$1.95 \cdot 10^{-2}$	–
A_2	$1.00 \cdot 10^1$	$1.21 \cdot 10^2$	$4.51 \cdot 10^{-14}$	$1.01 \cdot 10^0 - 4.04 \cdot 10^1$	$6.34 \cdot 10^0$	$3.94 \cdot 10^{-3}$
	$1.00 \cdot 10^2$	$1.02 \cdot 10^4$	$5.33 \cdot 10^{-14}$	$9.75 \cdot 10^{-1} - 3.19 \cdot 10^1$	$5.37 \cdot 10^0$	$5.57 \cdot 10^{-2}$
	$1.00 \cdot 10^3$	$1.00 \cdot 10^6$	$3.95 \cdot 10^{-14}$	$9.65 \cdot 10^{-1} - 2.73 \cdot 10^1$	$4.88 \cdot 10^0$	$5.61 \cdot 10^0$
	$1.00 \cdot 10^4$	$1.00 \cdot 10^8$	$3.79 \cdot 10^{-14}$	$9.49 \cdot 10^{-1} - 2.85 \cdot 10^1$	$4.96 \cdot 10^0$	$3.35 \cdot 10^2$
	$1.00 \cdot 10^5$	$1.00 \cdot 10^{10}$	–	$9.61 \cdot 10^{-1} - 3.65 \cdot 10^1$	$5.48 \cdot 10^0$	–
	$1.00 \cdot 10^7$	$1.00 \cdot 10^{14}$	–	$9.62 \cdot 10^{-1} - 3.73 \cdot 10^1$	$5.55 \cdot 10^0$	–
A_3	$1.00 \cdot 10^1$	$1.21 \cdot 10^2$	$2.86 \cdot 10^{-14}$	$4.27 \cdot 10^{-2} - 1.67 \cdot 10^0$	$2.46 \cdot 10^{-1}$	$3.32 \cdot 10^{-3}$
	$1.00 \cdot 10^2$	$1.02 \cdot 10^4$	$5.83 \cdot 10^{-14}$	$3.69 \cdot 10^{-2} - 4.11 \cdot 10^{-1}$	$1.26 \cdot 10^{-1}$	$5.59 \cdot 10^{-2}$
	$1.00 \cdot 10^3$	$1.00 \cdot 10^6$	$5.92 \cdot 10^{-14}$	$3.65 \cdot 10^{-2} - 3.89 \cdot 10^{-1}$	$1.26 \cdot 10^{-1}$	$3.76 \cdot 10^0$
	$1.00 \cdot 10^4$	$1.00 \cdot 10^8$	$4.29 \cdot 10^{-14}$	$3.60 \cdot 10^{-2} - 5.46 \cdot 10^{-1}$	$1.27 \cdot 10^{-1}$	$3.53 \cdot 10^2$
	$1.00 \cdot 10^5$	$1.00 \cdot 10^{10}$	–	$3.64 \cdot 10^{-2} - 7.33 \cdot 10^{-1}$	$1.63 \cdot 10^{-1}$	–
	$1.00 \cdot 10^7$	$1.00 \cdot 10^{14}$	–	$3.64 \cdot 10^{-2} - 5.74 \cdot 10^{-1}$	$1.41 \cdot 10^{-1}$	–
A_4	$4.00 \cdot 10^0$	$1.25 \cdot 10^2$	$6.41 \cdot 10^{-13}$	$5.25 \cdot 10^0 - 1.49 \cdot 10^2$	$2.64 \cdot 10^1$	$1.34 \cdot 10^{-2}$
	$2.20 \cdot 10^1$	$1.22 \cdot 10^4$	$3.24 \cdot 10^{-13}$	$4.84 \cdot 10^0 - 1.54 \cdot 10^2$	$2.60 \cdot 10^1$	$1.54 \cdot 10^{-1}$
	$1.00 \cdot 10^2$	$1.03 \cdot 10^6$	$2.83 \cdot 10^{-13}$	$2.02 \cdot 10^0 - 1.34 \cdot 10^2$	$1.87 \cdot 10^1$	$7.10 \cdot 10^0$
	$4.64 \cdot 10^2$	$1.01 \cdot 10^8$	–	$2.02 \cdot 10^0 - 1.43 \cdot 10^2$	$1.69 \cdot 10^1$	–
	$2.20 \cdot 10^3$	$1.07 \cdot 10^{10}$	–	$2.02 \cdot 10^0 - 1.81 \cdot 10^2$	$1.63 \cdot 10^1$	–
	$4.64 \cdot 10^4$	$9.99 \cdot 10^{13}$	–	$2.01 \cdot 10^0 - 1.94 \cdot 10^2$	$1.73 \cdot 10^1$	–
A_5	$4.00 \cdot 10^0$	$1.25 \cdot 10^2$	$2.90 \cdot 10^{-13}$	$1.25 \cdot 10^0 - 2.67 \cdot 10^1$	$4.82 \cdot 10^0$	$1.85 \cdot 10^{-2}$
	$2.20 \cdot 10^1$	$1.22 \cdot 10^4$	$1.87 \cdot 10^{-13}$	$9.38 \cdot 10^{-1} - 2.07 \cdot 10^1$	$4.22 \cdot 10^0$	$1.78 \cdot 10^{-1}$
	$1.00 \cdot 10^2$	$1.03 \cdot 10^6$	$1.73 \cdot 10^{-13}$	$1.05 \cdot 10^{-1} - 1.42 \cdot 10^1$	$1.46 \cdot 10^0$	$8.19 \cdot 10^0$
	$4.64 \cdot 10^2$	$1.01 \cdot 10^8$	–	$1.05 \cdot 10^{-1} - 8.31 \cdot 10^0$	$8.44 \cdot 10^{-1}$	–
	$2.20 \cdot 10^3$	$1.07 \cdot 10^{10}$	–	$1.05 \cdot 10^{-1} - 7.52 \cdot 10^0$	$8.41 \cdot 10^{-1}$	–
	$4.64 \cdot 10^4$	$9.99 \cdot 10^{13}$	–	$1.05 \cdot 10^{-1} - 7.36 \cdot 10^0$	$8.37 \cdot 10^{-1}$	–

TABLE 4. The performance and accuracy of our algorithm, compared to naive summation, for the lattices described by the parameter m and the lattice matrices defined in Table 3.

We demonstrate the effect of increasing the condition number of the matrix A , reporting the error $E = \min(E_{\text{abs}}, E_{\text{rel}})$ evaluated at $\mathbf{x} = A(-\frac{1}{2})_{j=1}^d$ and $\mathbf{y} = 0$, for $\nu = d + 0.1$, with the lattice L with $m = 10^2$ in $d = 2$ dimensions, and the lattice L with $m = 22$ in $d = 3$ dimensions, for the matrices

$$A = \begin{pmatrix} 1 & 0 \\ 1 & 1/\mu \end{pmatrix} \quad \text{and} \quad A = \begin{pmatrix} 1 & 0 & 0 \\ 1 & 1/\mu & 0 \\ 0 & 0 & 1 \end{pmatrix},$$

since for both of these matrices $\kappa(A) \approx \mu$. For $d = 2$, we let μ vary over 201 equispaced values between 1 and 200; for $d = 3$, we let μ vary over 201 equispaced values between 1 and 10. We also report the runtime t in seconds. The results are shown in Fig. 6. The cost is seen to grow like $O(\kappa(A)^d)$, as mentioned in Section 7.1.

FIGURE 5. The error plotted for a range of ν , for $d = 1, 2, 3$.FIGURE 6. The errors (left) and runtimes (right) for a range of condition numbers $\kappa(A)$.

ACKNOWLEDGEMENTS

The authors gratefully acknowledge the scientific support and HPC resources provided by the Erlangen National High Performance Computing Center (NHR@FAU) of the Friedrich-Alexander-Universität Erlangen-Nürnberg (FAU) under the NHR project n101af. NHR funding is provided by federal and Bavarian state authorities. NHR@FAU hardware is partially funded by the German Research Foundation (DFG) – 440719683. TK acknowledges funding received from the European Union’s Horizon 2020 research and innovation programme under the Marie Skłodowska–Curie grant

agreement No 899987. KS's work was supported in part by the NSERC Discovery Grants RGPIN-2020-06022 and DGECR-2020-00356.



APPENDIX A. TECHNICAL LEMMAS

Here, we collect results that are needed to formulate the proofs of all theorems but that are not relevant for the understanding of the main results.

A.1. Properties of G_ν . We split the proof of our central theorem into several lemmas. The first ones are concerned with the properties of G_ν .

Proof of Lemma 6.11. The topology on $\mathcal{S}(\mathbb{R}^d)$ is generated by the seminorms

$$q_{\alpha,\beta}(\varphi) = \sup_{\mathbf{z} \in \mathbb{R}^d} |\mathbf{z}^\alpha \partial^\beta \varphi(\mathbf{z})|, \quad \alpha, \beta \in \mathbb{N}_0^d, \quad |\beta| \leq k.$$

To show convergence, we split \mathbb{R}^d into a compact set comprising the origin and an unbounded set. To that end, let $\chi \in \mathcal{D}(\mathbb{R}^d)$ with $\chi = 1$ on a neighborhood of $\mathbf{0}$. By the triangle inequality for seminorms,

$$q_{\alpha,\beta}(G_{-\mu} - \gamma_n) \leq q_{\alpha,\beta}(\chi G_{-\mu} - \chi \gamma_n) + q_{\alpha,\beta}((1 - \chi)G_{-\mu} - (1 - \chi)\gamma_n),$$

so we can study the bounded and unbounded case separately. For the latter, note that $(1 - \chi)G_{-\mu}$ and the sequence $(1 - \chi)\gamma_n$, $n \in \mathbb{N}_0$, are elements of $\mathcal{S}(\mathbb{R}^d)$, so by Lemma 6.8 it requires to show that

$$\lim_{n \rightarrow \infty} (1 - \chi(\mathbf{z}))\gamma_n(\mathbf{z}) = (1 - \chi(\mathbf{z}))G_{-\mu}(\mathbf{z}), \quad \mathbf{z} \in \mathbb{R}^d,$$

and that $((1 - \chi)\gamma_n)_n$ is bounded. The pointwise convergence follows immediately by noting that γ_n is a Riemann sum approximating $G_{-\mu}$. To show boundedness in $\mathcal{S}(\mathbb{R}^d)$, we use Lemma A.3, applied to

$$\varphi(\mathbf{z}) = \exp(-\pi|\mathbf{z}|^2), \quad \mathbf{z} \in \mathbb{R}^d$$

and note that

$$\gamma_n = \frac{1}{n} \sum_{j=1}^n (j/n)^{\mu-1} (1 - \chi)\varphi(\cdot/(j/n)),$$

so that if $(1 - \chi)\varphi(\cdot/t)$ is bounded by a constant $C > 0$ in a seminorm of $\mathcal{S}(\mathbb{R}^d)$, independently of $t > 0$, then γ_n is bounded by the same constant in the same seminorm. $\mathbf{0}$, $\bar{B}_1(\mathbf{0})$ and the rest, $\mathbb{R}^d \setminus \bar{B}_1(\mathbf{0})$.

Next, we turn to convergence of $\chi\gamma_n$ to $\chi G_{-\mu}$. By assumption on μ , $G_{-\mu}$ is k times continuously differentiable with

$$\partial^\beta G_{-\mu}(\mathbf{z}) = \sum_{|\delta| \leq |\beta|} c_\delta \int_0^1 2t^{\mu-|\beta|-1} (\mathbf{z}/t)^\delta \exp(-\pi|\mathbf{z}|^2/t^2) dt,$$

for some constants c_δ . With the same coefficients, it also holds

$$\partial^\beta \gamma_n(\mathbf{z}) = \sum_{|\delta| \leq |\beta|} c_\delta \frac{1}{n} \sum_{j=1}^n 2(j/n)^{\mu-|\beta|-1} (n/j\mathbf{z})^\delta \exp(-\pi n^2/j^2|\mathbf{z}|^2).$$

Thus, we can focus on the convergence of each summand. To that end, we study functions of the form $\eta : [0, 1] \times \mathbb{R}^d \rightarrow \mathbb{C}$ with

$$\eta(t, \mathbf{z}) = 2t^{\mu-|\beta|-1}(\mathbf{z}/t)^\delta \exp(-\pi|\mathbf{z}|^2/t^2)$$

for $t > 0$ and $\eta(0, \mathbf{z}) = 0$. The function η is continuous as factors including \mathbf{z} are always bounded uniformly in t , independently of δ , so that

$$|\eta(t, \mathbf{z})| \leq Ct^{\operatorname{Re}(\mu)-|\beta|-1},$$

for a constant $C > 0$, which tends to 0 as $t \rightarrow 0$, owing to the choice of μ and β . Multiplied with a smooth function of compact support it is uniformly continuous and hence the Riemann sums $\chi\gamma_n$ converge uniformly in all derivatives up to order k to $\chi G_{-\mu}$. \square

Lemma A.1. *Let $\beta > 0$. The Fourier transformation of the smooth function*

$$\mathbf{z} \mapsto \int_0^\beta 2t^{\nu-1} e^{-\pi\mathbf{z}^2 t^2} dt$$

for $\nu > d + 1$ is given by $\beta^{-d+\nu} G_{d-\nu}(\cdot/\beta)$.

Proof. Let $h : \mathbb{R}^d \rightarrow \mathbb{C}$ denote

$$h(\mathbf{z}) = \int_0^\beta 2t^{\nu-1} e^{-\pi\mathbf{z}^2 t^2} dt.$$

To compute the Fourier transform, we discretize the integral from 0 to β by a Riemann sum, which results in Schwartz functions

$$h_n(\mathbf{z}) = \frac{\beta}{n} \sum_{j=1}^n 2t_j^{\nu-1} e^{-\pi\mathbf{z}^2 t_j^2}, \quad t_j = \frac{\beta}{n} j.$$

Since the integrand is continuous, we have for each $\mathbf{z} \in \mathbb{R}^d$,

$$\lim_{n \rightarrow \infty} h_n(\mathbf{z}) = h(\mathbf{z}).$$

Additionally,

$$|h_n(\mathbf{z})| \leq \frac{\beta}{n} \sum_{j=1}^n t_j^{\nu-1}, \quad \mathbf{z} \in \mathbb{R}^d.$$

As the right-hand side converges to the integral of the continuous function $t \mapsto 2t^{\nu-1}$ over $[0, \beta]$, it is uniformly bounded in $n \in \mathbb{N}_0$. Thus, $(h_n)_n$ converges to h in $\mathcal{S}'(\mathbb{R}^d)$. In particular, the Fourier transformations of $(h_n)_n$ converge to $\mathcal{F}h$. The Fourier transformation is readily computed as

$$\mathcal{F}h_n(\mathbf{k}) = \frac{\beta}{n} \sum_{j=1}^n 2t_j^{\nu-d-1} e^{-\pi\mathbf{k}^2/t_j^2}, \quad \mathbf{k} \in \mathbb{R}^d.$$

By assumption, $\nu > d + 1$, so $t \mapsto 2t^{\nu-d-1}$ is continuous and bounded on $[0, \beta]$. Hence, $\mathcal{F}h_n(\mathbf{k})$ converges to

$$\int_0^\beta t^{\nu-d-1} e^{-\pi\mathbf{k}^2/t^2} dt = \beta^{-d+\nu} G_{d-\nu}(\mathbf{k}/\beta),$$

which proves the asserted form of $\mathcal{F}h$. \square

A.2. Hadamard representation. In the following we collect the necessary lemmas for the proof of Lemma 6.12.

Lemma A.2. *Let $\beta : [0, 1] \times \mathbb{R}^d \rightarrow \mathbb{C}$ be a smooth mapping such that for all $t \in [0, 1]$, $\beta(t, \cdot)$ is a Schwartz function. If the families of partial derivatives $t \mapsto \partial_t^k \beta(t, \cdot)$, $k \in \mathbb{N}_0$, are uniformly bounded in the Schwartz topology, then β is smooth as a mapping of $[0, 1]$ to $\mathcal{S}(\mathbb{R}^d)$,*

$$[0, 1] \rightarrow \mathcal{S}(\mathbb{R}^d), \quad t \mapsto \beta(t, \cdot),$$

and $\partial_t^k \beta(t, \cdot) \in \mathcal{S}(\mathbb{R}^d)$ for all $t \in [0, 1]$, $k \in \mathbb{N}_0$.

Proof. We focus on the first derivative. An inductive argument can be used to prove the assertion for an arbitrary derivative order. First, we write the finite difference as an integral,

$$\frac{\beta(t+h, \mathbf{z}) - \beta(t, \mathbf{z})}{h} = \int_0^1 \partial_t \beta(t+h\tau, \mathbf{z}) \, d\tau, \quad \mathbf{z} \in \mathbb{R}^d.$$

By assumption, the integral on the right hand side is uniformly bounded in t, h in all Schwartz seminorms. Thus, the finite difference is bounded too. Furthermore, the finite difference converges for fixed $\mathbf{z} \in \mathbb{R}^d$ to $\partial_t \beta(t, \mathbf{z})$. Owing to Lemma 6.8, it converges strongly in $\mathcal{S}(\mathbb{R}^d)$ with $\partial_t \beta(t, \cdot) \in \mathcal{S}(\mathbb{R}^d)$ for all $t \in [0, 1]$. \square

Lemma A.3. *For $\varphi \in \mathcal{S}(\mathbb{R}^d)$ and $\chi \in \mathcal{D}(\mathbb{R}^d)$ with $\chi = 1$ on a neighborhood of $\mathbf{0}$, the mapping*

$$\beta : [0, 1] \times \mathbb{R}^d \rightarrow \mathbb{C}, \quad (t, \mathbf{z}) \mapsto \begin{cases} (1 - \chi(\mathbf{z}))\varphi(\mathbf{z}/t), & t \neq 0 \\ 0, & t = 0 \end{cases}$$

is smooth as a mapping $[0, 1] \rightarrow \mathcal{S}(\mathbb{R}^d)$ with vanishing derivatives at $t = 0$. Furthermore, the Schwartz seminorms of $\partial_t^k \beta(t, \cdot)$, $k \in \mathbb{N}_0$, are uniformly bounded in $t \in [0, 1]$ by seminorms of φ .

Proof. First, we note that for any $t \in [0, 1]$, $\beta(t, \cdot)$ is a Schwartz function, so the mapping is well-defined. Moreover, it is a smooth function on $(0, 1] \times \mathbb{R}^d$. Its partial derivatives are linear combinations of

$$(t, \mathbf{z}) \mapsto \partial^\alpha (1 - \chi)(\mathbf{z}) t^{-n} \mathbf{z}^\delta \partial^\gamma \varphi(\mathbf{z}/t),$$

for $\alpha, \gamma, \delta \in \mathbb{N}_0^d$ and $n \in \mathbb{N}_0$. To prove differentiability for $t = 0$, we claim that all derivatives in $t = 0$ vanish and consider the finite difference of above term for $\mathbf{z} \in \mathbb{R}^d$,

$$\lim_{t \rightarrow 0} \frac{\partial^\alpha (1 - \chi)(\mathbf{z}) t^{-n} \mathbf{z}^\delta \partial^\gamma \varphi(\mathbf{z}/t)}{t} = \lim_{t \rightarrow 0} \partial^\alpha (1 - \chi)(\mathbf{z}) t^{-n-1} \mathbf{z}^\delta \partial^\gamma \varphi(\mathbf{z}/t).$$

The limit can be rewritten as

$$\begin{aligned} & \lim_{t \rightarrow 0} \partial^\alpha (1 - \chi)(\mathbf{z}) t^{-n-1} \mathbf{z}^\delta \partial^\gamma \varphi(\mathbf{z}/t) \\ &= \lim_{t \rightarrow 0} t^{|\delta|+1} \frac{\partial^\alpha (1 - \chi)(\mathbf{z})}{z_1^{n+2}} (z_1/t)^{n+2} (z/t)^\delta \partial^\gamma \varphi(\mathbf{z}/t), \end{aligned}$$

where the term involving χ is zero already on a neighborhood of zero. In particular, this a smooth and bounded function on \mathbb{R}^d , regardless of the singular $1/z_1^{n+2}$ at the

origin. Hence, we can bound the term as

$$\begin{aligned} & \left| t^{|\delta|+1} \frac{\partial^\alpha(1-\chi)(\mathbf{z})}{z_1^{n+2}} (z_1/t)^{n+2} (z/t)^\delta \partial^\gamma \varphi(z/t) \right| \\ & \leq t^{|\delta|+1} \sup_{\mathbf{x} \in \mathbb{R}^d} \left| \frac{\partial^\alpha(1-\chi)(\mathbf{x})}{x_1^{n+2}} \right| \sup_{\mathbf{x} \in \mathbb{R}^d} |x_1^{n+2} \mathbf{x}^\delta \partial^\gamma \varphi(\mathbf{x})|, \end{aligned}$$

so that the limit $t \rightarrow 0$ is zero. Therefore, β is smooth on $[0, 1] \times \mathbb{R}^d$ and all partial derivatives vanish at $t = 0$. Moreover, above estimates show that Schwartz seminorms with respect to \mathbf{z} of all partial derivatives of β are uniformly bounded for $t \in [0, 1]$ in terms of Schwartz seminorms of φ . The assertion now follows from Lemma A.3. \square

Proof of Lemma 6.12. For $\mathbf{y}_0 \in U$ there exists an open neighborhood $\Omega \subseteq U$ of \mathbf{y}_0 and $\varepsilon > 0$ such that $\mathbf{y} + B_{3\varepsilon}(\mathbf{0}) \subseteq U$ for all $\mathbf{y} \in \Omega$. Hence, for $\chi \in \mathcal{D}(\mathbb{R}^d)$ even with $\text{supp } \chi \subseteq B_{2\varepsilon}(\mathbf{0})$, $0 \leq \chi \leq 1$, and $\chi = 1$ on $B_\varepsilon(\mathbf{0})$, the distribution $\tau_{\mathbf{y}}\chi u$ is a smooth function with compact support for every $\mathbf{y} \in \Omega$. If we split $T\varphi$ into two parts,

$$T\varphi(t, \mathbf{y}) = ([\tau_{\mathbf{y}}\chi u] * \varphi(\cdot/t))(\mathbf{y}) + ((1 - \tau_{\mathbf{y}}\chi)u) * \varphi(\cdot/t)(\mathbf{y}),$$

then for first term, denoted by $T_1\varphi$, we have

$$T_1\varphi(t, \mathbf{y}) = t^d \int_{\mathbb{R}^d} \chi(t\mathbf{z})u(\mathbf{y} - t\mathbf{z})\varphi(\mathbf{z}) \, d\mathbf{z}, \quad t \geq 0, \mathbf{y} \in \Omega.$$

Owing to the choice of the cut-off function χ ,

$$|\chi(t\mathbf{z})u(\mathbf{y} - t\mathbf{z})| \leq \sup_{\mathbf{z} \in \Omega + B_{2\varepsilon}(\mathbf{0})} |u(\mathbf{z})|.$$

Similar bounds also hold for arbitrary derivatives with respect to t and \mathbf{y} of the integrand. By the dominated convergence theorem, $T_1\varphi$ is a smooth function of both arguments. Furthermore, $T_1\varphi$ is bounded by

$$|T_1\varphi(t, \mathbf{y})| \leq \sup_{\mathbf{z} \in \Omega + B_{2\varepsilon}(\mathbf{0})} |u(\mathbf{z})| \sup_{\mathbf{z} \in \mathbb{R}^d} |(1 + |\mathbf{z}|^2)^d \varphi(\mathbf{z})| \int_{\mathbb{R}^d} (1 + |\mathbf{z}|^2)^{-d} \, d\mathbf{z},$$

and similarly for its derivatives. This proves that T_1 is a continuous linear mapping of $\mathcal{S}(\mathbb{R}^d)$ to $C^\infty([0, 1] \times \Omega)$. Since \mathbf{y} was arbitrary, the smoothness around any point of U implies that T_1 maps onto smooth functions on the whole complement of the singular support, that is

$$T_1 : \mathcal{S}(\mathbb{R}^d) \rightarrow C^\infty([0, 1] \times U)$$

is well-defined, linear and continuous.

We now focus on the second term, $T_2\varphi$. Since χ is even, the convolution in $T_2\varphi$ can be rewritten as

$$T_2\varphi(t, \mathbf{y}) = u * [(1 - \chi)\varphi(\cdot/t)](\mathbf{y}) = [u * \beta(t, \cdot)](\mathbf{y})$$

with $\beta(t, \mathbf{z}) = (1 - \chi(\mathbf{z}))\varphi(\mathbf{z}/t)$. For any $t \in [0, 1]$, $\beta(t, \cdot)$ is a Schwartz function, so the convolution is a smooth function of \mathbf{y} . Furthermore, for fixed $\mathbf{y} \in \mathbb{R}^d$, the convolution is a smooth function of $t \in [0, 1]$ by Lemma A.3. Thus, $T_2\varphi \in C^\infty([0, 1] \times \mathbb{R}^d)$. To show continuity of the mapping, we observe that any partial derivative of degree k in t and of arbitrary order in \mathbf{y} is bounded compactly in \mathbf{y} by seminorms of $\partial_t^k \beta(t, \cdot)$, that, by Lemma A.3, are uniformly bounded in t by seminorms of φ . Thus, $T_2\varphi$ is bounded and consequently continuous.

We conclude with a proof of the addendum for an even test function φ . For $t \in [-1, 1]$, $t \neq 0$, we have

$$\varphi(\mathbf{z}/t) = \varphi(\mathbf{z}/|t|), \quad \mathbf{z} \in \mathbb{R}^d.$$

In particular, we can smoothly extend $T_2\varphi$ from $(0, 1]$ to $[-1, 1] \setminus \{0\}$ via

$$T_2\varphi(t, \mathbf{y}) = T_2\varphi(|t|, \mathbf{y}).$$

For continuation into $t = 0$ we note that all derivatives of $T_2\varphi$ decay super-algebraically for $t \rightarrow 0$ as a result of the proof for Lemma A.3. Hence the function

$$g(t, \mathbf{y}) = |t|^{-d} T_2\varphi(|t|, \mathbf{y}), \quad t \in [-1, 1] \setminus \{0\}, \quad \mathbf{y} \in \mathbb{R}^d$$

has a smooth extension for $t = 0$ with $g^{(k)}(0) = 0$ for all $k \in \mathbb{N}_0$. This shows

$$g(t, \mathbf{y}) = \eta_2(t^2, \mathbf{y}), \quad t \in [-1, 1], \quad \mathbf{y} \in \mathbb{R}^d,$$

for $\eta \in C^\infty([0, 1] \times \mathbb{R}^d)$, so that

$$T_2\varphi(t, \mathbf{y}) = t^d \eta_2(t^2, \mathbf{y}), \quad t \in [0, 1].$$

Because φ is even, we can write

$$\int_{\mathbb{R}^d} \chi(t(-\mathbf{z})) u(\mathbf{y} - t(-\mathbf{z})) \varphi(\mathbf{z}) \, d\mathbf{z} = \int_{\mathbb{R}^d} \chi(t\mathbf{z}) u(\mathbf{y} - t\mathbf{z}) \varphi(\mathbf{z}) \, d\mathbf{z}$$

for $t \in [0, 1]$, $\mathbf{y} \in \Omega$, which shows that

$$T_1(t, \mathbf{y}) = t^d v(t, \mathbf{y}), \quad t \in [0, 1], \quad \mathbf{y} \in U,$$

for an even, smooth function v . Hence, there is $\eta_1 \in C^\infty([0, 1] \times U)$ such that

$$T_1\varphi(t, \mathbf{y}) = t^d \eta_1(t^2, \mathbf{y}).$$

The combination of both results proves the desired assertion. \square

REFERENCES

- [1] Morteza Aghaee et al. “InAs-Al hybrid devices passing the topological gap protocol”. In: *Physical Review B* 107.24 (2023), p. 245423. URL: <https://doi.org/10.1103/PhysRevB.107.245423>.
- [2] T. M. Apostol. *Introduction to Analytic Number Theory*. Undergraduate Texts in Mathematics. Springer New York, 1998.
- [3] J. Borwein et al. *Lattice Sums Then and Now*. Encyclopedia of Mathematics and its Applications. Cambridge University Press, 2013. URL: <https://doi.org/10.1017/CB09781139626804>.
- [4] S. T. Bramwell et al. “Measurement of the charge and current of magnetic monopoles in spin ice”. In: *Nature* 461.7266 (Oct. 2009), pp. 956–959. URL: <https://doi.org/10.1038/nature08500>.
- [5] Steven T Bramwell and Michel JP Gingras. “Spin ice state in frustrated magnetic pyrochlore materials”. In: *Science* 294.5546 (2001), pp. 1495–1501. URL: <https://doi.org/10.1126/science.1064761>.
- [6] Steven T Bramwell and Mark J Harris. “The history of spin ice”. In: *J. Phys.: Condens. Matter* 32.37 (June 2020), p. 374010. URL: <https://doi.org/10.1088/1361-648x/ab8423>.

- [7] Andreas A Buchheit and Torsten Keßler. “On the Efficient Computation of Large Scale Singular Sums with Applications to Long-Range Forces in Crystal Lattices”. In: *J. Sci. Comput.* 90.1 (2022), pp. 1–20. DOI: 10.1007/s10915-021-01731-5. URL: <https://doi.org/10.1007/s10915-021-01731-5>.
- [8] Andreas A Buchheit and Torsten Keßler. “Singular Euler–Maclaurin expansion on multidimensional lattices”. In: *Nonlinearity* 35.7 (2022), p. 3706.
- [9] Andreas A Buchheit et al. “Exact Continuum Representation of Long-range Interacting Systems and Emerging Exotic Phases in Unconventional Superconductors”. In: *arXiv preprint arXiv:2201.11101v3* (2023).
- [10] Andreas A. Buchheit and T. Keßler. *GitHub release: Continuum representation 2.2*. 2023. URL: <https://doi.org/10.5281/zenodo.7575976>.
- [11] A. Campa et al. *Physics of long-range interacting systems*. OUP Oxford, 2014.
- [12] C. Castelnovo, R. Moessner, and S. L. Sondhi. “Magnetic monopoles in spin ice”. In: *Nature* 451.7174 (Jan. 2008), pp. 42–45. URL: <https://doi.org/10.1038/nature06433>.
- [13] Shukai Chen, Kirill Serkh, and James Bremer. “The adaptive Levin method”. In: *arXiv preprint arXiv:2211.13400* (2022).
- [14] Sarvadaman Chowla and Atle Selberg. “On Epstein’s zeta function (I)”. In: *Proceedings of the National Academy of Sciences* 35.7 (1949), pp. 371–374. URL: <https://doi.org/10.1073/pnas.35.7.371>.
- [15] R. Crandall. “Unified algorithms for polylogarithm, L-series, and zeta variants”. In: *Algorithmic Reflections: Selected Works*. PSIPress, 2012.
- [16] E Elizalde. “Multidimensional extension of the generalized Chowla–Selberg formula”. In: *Communications in mathematical physics* 198.1 (1998), pp. 83–95.
- [17] Emilio Elizalde. *Ten physical applications of spectral zeta functions*. Vol. 855. Springer, 2012.
- [18] O. Emersleben. “Zetafunktionen und elektrostatische Gitterpotentiale. I”. In: *Phys. Z* 24 (1923), pp. 73–80.
- [19] O. Emersleben. “Zetafunktionen und elektrostatische Gitterpotentiale. II”. In: *Phys. Z* 24 (1923), pp. 97–104.
- [20] P. Epstein. “Zur Theorie allgemeiner Zetafunktionen”. In: *Math. Ann.* 56 (1903), pp. 615–644. URL: <https://doi.org/10.1007/BF01444309>.
- [21] P. Epstein. “Zur Theorie allgemeiner Zetafunktionen. II”. In: *Math. Ann.* 63 (1906), pp. 205–216. URL: <https://doi.org/10.1007/BF01449900>.
- [22] S. Fey, S. C. Kapfer, and K. P. Schmidt. “Quantum criticality of two-dimensional quantum magnets with long-range interactions”. In: *Phys. Rev. Lett.* 122.1 (2019), p. 017203. URL: <https://doi.org/10.1103/PhysRevLett.122.017203>.
- [23] Giovanni Finocchio et al. “The promise of spintronics for unconventional computing”. In: *Journal of Magnetism and Magnetic Materials* 521 (2021), p. 167506.
- [24] Hongmin Gao, Frank Schlawin, and Dieter Jaksch. “Higgs mode stabilization by photoinduced long-range interactions in a superconductor”. In: *Physical Review B* 104.14 (2021), p. L140503. URL: <https://doi.org/10.1103/PhysRevB.104.L140503>.
- [25] I. M. Gel’fand and G. E. Shilov. *Generalized Functions. Volume I. Properties and Operations*. Academic Press, 1964.

- [26] Amparo Gil, Javier Segura, and Nico M Temme. “Efficient and accurate algorithms for the computation and inversion of the incomplete gamma function ratios”. In: *SIAM Journal on Scientific Computing* 34.6 (2012), A2965–A2981.
- [27] M. Glasser. “The evaluation of lattice sums. I. Analytic procedures”. In: *J. Math. Phys.* 14.3 (1973), pp. 409–413. URL: <https://doi.org/10.1063/1.1666331>.
- [28] M. Glasser. “The evaluation of lattice sums. II. Number-theoretic approach”. In: *J. Math. Phys.* 14.6 (1973), pp. 701–703.
- [29] Stephen W Hawking. “Zeta function regularization of path integrals in curved spacetime”. In: *Communications in Mathematical Physics* 55 (1977), pp. 133–148. URL: <https://doi.org/10.1007/BF01626516>.
- [30] Johan Helsing and Rikard Ojala. “On the evaluation of layer potentials close to their sources”. In: *Journal of Computational Physics* 227.5 (2008), pp. 2899–2921.
- [31] J. Horváth. *Topological Vector Spaces and Distributions*. Reprinted by Dover, 2012. Addison–Wesley Publications, 1966.
- [32] Steven G. Johnson. *Faddeeva Package*. http://ab-initio.mit.edu/wiki/index.php/Faddeeva_Package. Accessed: June 5, 2023. 2012.
- [33] Frans Lemeire. “Bounds for condition numbers of triangular and trapezoid matrices”. In: *BIT Numerical Mathematics* 15.1 (1975), pp. 58–64.
- [34] Roman M Lutchny et al. “Majorana zero modes in superconductor–semiconductor heterostructures”. In: *Nature Reviews Materials* 3.5 (2018), pp. 52–68. URL: <https://doi.org/10.1038/s41578-018-0003-1>.
- [35] JC Martinez et al. “Theory of current-induced skyrmion dynamics close to a boundary”. In: *Journal of Magnetism and Magnetic Materials* 465 (2018), pp. 685–691.
- [36] D. O’Dell et al. “Bose-Einstein Condensates with $1/r$ Interatomic Attraction: Electromagnetically Induced “Gravity””. In: *Phys. Rev. Lett.* 84 (25 June 2000), pp. 5687–5690. URL: <https://doi.org/10.1103/PhysRevLett.84.5687>.
- [37] Ch. Psaroudaki and Ch. Panagopoulos. “Skyrmion qubits: A new class of quantum logic elements based on nanoscale magnetization”. In: *Phys. Rev. Lett.* 127.6 (2021), p. 067201. URL: <https://doi.org/10.1103/PhysRevLett.127.067201>.
- [38] P. Richerme et al. “Non-local propagation of correlations in quantum systems with long-range interactions”. In: *Nature* 511.7508 (July 2014), pp. 198–201. URL: <https://doi.org/10.1038/nature13450>.
- [39] Daniel Shanks. “Calculation and applications of Epstein zeta functions”. In: *Mathematics of Computation* 29.129 (1975), pp. 271–287. URL: <https://doi.org/10.1090/S0025-5718-1975-0409357-2>.
- [40] Zewen Shen and Kirill Serkh. “Is polynomial interpolation in the monomial basis unstable?” In: *arXiv preprint arXiv:2212.10519* (2022).
- [41] K. M. Song et al. “Skyrmion-based artificial synapses for neuromorphic computing”. In: *Nat. Electron.* 3.3 (2020), pp. 148–155. URL: <https://doi.org/10.1038/s41928-020-0385-0>.
- [42] A. Terras. *Harmonic Analysis on Symmetric Spaces and Applications I*. Springer New York, 2012. ISBN: 9781461251286. URL: <https://doi.org/10.1007/978-1-4612-5128-6>.

- [43] Audrey A Terras. “Bessel series expansions of the Epstein zeta function and the functional equation”. In: *Transactions of the American Mathematical Society* 183 (1973), pp. 477–486. URL: <https://doi.org/10.1090/S0002-9947-1973-0323735-6>.
- [44] F. Trèves. *Topological Vector Spaces, Distributions and Kernels*. Reprinted by Dover, 2006. Academic Press, 1967.
- [45] X. Zhang et al. “Skyrmion dynamics in a frustrated ferromagnetic film and current-induced helicity locking-unlocking transition”. In: *Nat. Commun.* 8.1 (2017), pp. 1–10. URL: <https://doi.org/10.1038/s41467-017-01785-w>.
- [46] I.J. Zucker. “The Exact Evaluation of Some New Lattice Sums”. In: *Symmetry* 9.12 (2017), p. 314. URL: <https://doi.org/10.3390/sym9120314>.

2

DEPARTMENT OF MATHEMATICS, SAARLAND UNIVERSITY, 66123 SAARBRÜCKEN, GERMANY
Email address: buchheit@num.uni-sb.de

DEPARTMENT OF MECHANICAL ENGINEERING, EINDHOVEN UNIVERSITY OF TECHNOLOGY, 5600 MB EINDHOVEN, NETHERLANDS

DEPARTMENTS OF MATHEMATICS AND COMPUTER SCIENCE, UNIVERSITY OF TORONTO, TORONTO, ON M5S 2E4, CANADA